

UNCLASSIFIED

AD. 461769L

DEFENSE DOCUMENTATION CENTER

FOR

SCIENTIFIC AND TECHNICAL INFORMATION

CAMERON STATION ALEXANDRIA, VIRGINIA



UNCLASSIFIED

NOTICE: When government or other drawings, specifications or other data are used for any purpose other than in connection with a definitely related government procurement operation, the U. S. Government thereby incurs no responsibility, nor any obligation whatsoever; and the fact that the Government may have formulated, furnished, or in any way supplied the said drawings, specifications, or other data is not to be regarded by implication or otherwise as in any manner licensing the holder or any other person or corporation, or conveying any rights or permission to manufacture, use or sell any patented invention that may in any way be related thereto.

CATALOGED BY: DDC

AS AD NO. 461769

L

Contract NONR 3437(00)

Semiannual Technical Summary Report

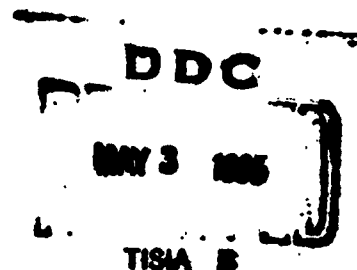
Period Ending 19 February 1965

"STABLE DENSE COLD PLASMA"

Advanced Research Projects Agency
Order No. 194, Amendment No. 5
Program Code No. 4980
Contract Date 20 February 1961, Completion 19 September 1965
Issued in Amount of \$507,995, as Amended

Project Scientist: Dr. S. Naiditch

Reproduction in whole or in part
permitted for any purpose of the
United States Government



UNIFIED SCIENCE ASSOCIATES, INC.

826 south arroyo parkway

pasadena, california

murray 1-3486

461769L

Contract NONR 3437(00)

Distribution List for Semiannual
and Final Technical Summary Reports

<u>Agency</u>	<u>No. of Copies</u>
Director, Advanced Research Projects Agency The Pentagon Washington, 25, D.C.	6
Chief of Naval Research Department of the Navy Washington, 25, D.C. Attn: Code 429	2
Commanding Officer Office of Naval Research Branch Office 1030 East Green Street Pasadena, 1, California	1
Chief, Bureau of Naval Weapons Department of the Navy Washington, 25, D.C. Attn: RRRE-6 RAPP-33 RAAE-511 DLI-3	1 1 1 1
Space Sciences Laboratory Litton Systems, Inc. Beverly Hills, California	1
AVCO-Everett Research Laboratory Everett, Massachusetts	1
Plasma Propulsion Laboratory Republic Aviation Corporation Farmingdale, New York	1
Stevens Institute of Technology Hoboken, New Jersey Attn: Winston H. Bostick	1
Astro Electronics Division RCA Laboratories Radio Corporation of America Princeton, New Jersey	1

<u>Agency</u>	<u>No. of Copies</u>
Allison Division General Motors Corporation Indianapolis, Indiana	1
Research Laboratories United Aircraft Corporation East Hartford, 8, Connecticut	1
Cambridge Research Laboratory L.G. Hanscom Field Bedford, Massachusetts	1
Electro-Optical Systems, Inc. 125 North Vinedo Avenue Pasadena, California	1
Space Sciences Laboratory Missile and Space Vehicle Dept. General Electric Company Philadelphia, 24, Pennsylvania	1
Geophysics Research and Development Center University of Maryland College Park, Maryland	1
Plasma Flow Section NASA, Lewis Research Center Cleveland, 35, Ohio	1
Experimental Physics Dept. Aeronutronics Ford Motor Company Newport Beach, California	1
California Institute of Technology 1201 East California Street Pasadena, California Attn: Robert G. Jahn	1
Plasmadyne Corporation Santa Ana, California	1
The Pennsylvania State University University Park, Pennsylvania Attn: Dr. H. Li	1
Gas Dynamic Laboratory Northwestern University Evanston, Illinois Attn: Dr. Ali Cambel	1

<u>Agency</u>	<u>No. of Copies</u>
Physics and Advanced Systems Dept. Reaction Motors Division Thiokol Chemical Corporation Denville, New Jersey	1
Atlantic Research Corporation Alexandria, Virginia	1
Armed Services Technical Information Agency Arlington Hall Station Arlington, 12, Virginia	10
Office of Technical Services Department of Commerce Washington, 25, D.C.	1
Professor E. Charles Evers Associate Professor of Chemistry University of Pennsylvania Philadelphia, Pennsylvania	1
Hughes Research Laboratories 3011 Malibu Canyon Road Malibu, California Attn: Dr. R. C. Knechtli	1
Rocket Power-Talco 3016 East Foothill Boulevard Pasadena, California Attn: Mr. M. Farber	1
Cambridge Research Laboratories Bedford, Massachusetts Attn: Code CKZAP, Dr. Norman Rosenberg	1
ASWMP-1 Aeronautical Systems Division Air Force Systems Command Wright-Patterson Air Force Base, Ohio Attn: K. E. Vickers, or 2nd Lt Carl N. Caputo	1
Professor J. C. Thompson University of Texas Austin, 12, Texas	1
Chief, Library NASA-Lewis Research Center 21000 Brookpark Road Cleveland, Ohio 44135	1

Contract NONR 3437(30)

<u>Agency</u>	<u>No. of Copies</u>
Mr. Jack A. Myers Westinghouse Electric Corporation P. O. Box 746 Baltimore 3, Maryland	1
Dr. D. C. Himes, Chief Physical Chem. Research Battelle Memorial Institute 505 King Avenue Columbus, Ohio 43201	1
Dr. Manfred Altman, Director Institute of Direct Energy Conversion University of Pennsylvania 113 Towne Building Philadelphia, Pennsylvania 19104	1
Mr. W. E. Emmerich Westinghouse Research Lab. Central Laboratories Churchill Borough Pittsburgh 35, Pennsylvania	1
Dr. S. Golden Department of Chemistry Brandeis University Waltham, Massachusetts	1
Mr. Derek W. Manaffey Staff Member Plasma Physics Laboratory Boeing Scientific Research Lab. P. O. Box 3931 Seattle 24, Washington	1

Contract NONR 3437(00)

Semiannual Technical Summary Report

Period Ending 19 February 1965

"STABLE DENSE COLD PLASMA"

Advanced Research Projects Agency
Order No. 194, Amendment No. 5
Program Code No. 4980
Contract Date 20 February 1961, Completion 19 September 1965
Issued in Amount of \$507,995, as Amended

Project Scientist: Dr. S. Naiditch

Reproduction in whole or in part
permitted for any purpose of the
United States Government

UNIFIED SCIENCE ASSOCIATES, INC.

826 south arroyo parkway

pasadena, california

murray 1-3486

TABLE OF CONTENTS

- 1.0 Abstract
- 2.0 Publications and Conferences
- 3.0 Hall Effect
 - 3.1 Introduction
 - 3.2 Experimental
 - 3.2.1 First Attempt at Measuring the Hall Coefficient of Mercury
 - 3.2.2 Efforts to Reduce the Noise Level by Improved Filter Circuits
 - 3.2.3 Effect of the Improved Filter Circuit on the Noise Level
 - 3.2.4 Effect of Intermodulation
 - 3.2.5 Hall Effect Measurement on a Cell with Electrodes
 - 3.3 Conclusions
 - 3.4 Program for the Next Period
 - 3.5 References
- 4.0 Magnetic Susceptibility of Sodium-Ammonia Solutions
 - 4.1 Introduction
 - 4.2 Experimental
 - 4.2.1 Design of the Apparatus
 - 4.2.2 Measurement of Magnetic Susceptibilities
 - 4.3 Conclusion
 - 4.4 Program for the Next Period
 - 4.5 References
- 5.0 Research on Surface Contaminants
 - 5.1 Introduction
 - 5.2 Experimental
 - 5.2.1 Elimination of Surface Contamination
 - 5.2.2 Effectiveness of Ammonia Purification
 - 5.2.3 Effect of Added Contaminants

5.3 Conclusions

5.4 Program for the Next Period

5.5 References

6.0 Chemical Analysis of Sodium-Ammonia Solutions
and Solubilities of Salts

6.1 Introduction

6.2 Experimental

6.2.1 Chemical Analysis of Sodium Ammonia

6.2.2 Solubility of Salts

6.3 Conclusions

6.4 Program for the Next Period

6.5 References

1.0 ABSTRACT

The purpose of this contract is to conduct research on chemical and physical properties of sodium ammonia solutions relating to their plasma aspects.

During the period of this report chemical studies were conducted in order to increase the lifetime of the solutions at elevated temperatures. This work included investigating effects of surface contaminants and solvent purification on the decomposition of sodium ammonia solutions. Quantitative measurements have been made to determine the effectiveness of various cleaning procedures for glass surfaces. A search was conducted for contaminants other than water which cause decomposition of the solution. Among the investigated contaminants, tungsten has the strongest effect.

Procedures for chemical analysis of sodium ammonia solutions were developed. The analysis confirmed the stability of sodium ammonia solutions up to 160°C and agreed fairly well with our conductivity data. Studies on salts in contact with sodium ammonia solutions were carried out.

The electrodeless Hall effect apparatus under development to provide data on electron densities and mobilities, was used to measure the Hall coefficient of mercury. This experiment was primarily considered as a final test of the apparatus. Unexpected difficulties were encountered from pickup noise and intermodulation. It was possible to overcome the disturbing effects on the measuring circuit sufficiently that Hall effect measurements on a cell with electrodes could be performed. The measured result was in fairly good agreement with the literature.

An apparatus for measuring magnetic susceptibilities of sodium ammonia solutions was devised. The functioning of the apparatus was tested by measuring the magnetic susceptibility of distilled water. First measurements on ammonia and sodium ammonia solutions were performed at room temperature.

2.0 PUBLICATIONS AND CONFERENCES

- 2.1 S. Naiditch presented a paper, "Dense Gaseous Cold Plasmas", at the Pasadena Meeting of the American Physical Society, Division of Fluid Dynamics, on November 25, 1964. The abstract follows.
- 2.2 A paper by R. A. Williams, E. M. Gold and S. Naiditch, on "The Two Transformer Method for Electrodeless Conductivity Measurement", has been submitted to the Review of Scientific Instruments, and accepted for publication, contingent on minor revisions. A copy of the original paper is being transmitted with this report.
- 2.3 S. Naiditch presented a seminar on "Conductivity of Sodium-Ammonia Solutions", at the Joint Meeting of the Southern California-Nevada Section of the Electrochemical Society and the UCLA Theoretical Electrochemistry and Corrosion Group on February 17, 1965.
- 2.4 A paper on Densities of Sodium-Ammonia Solutions is being prepared, and will be distributed shortly.
- 2.5 Dr. Mahaffey and Dr. Jerde of the Boeing Scientific Research Laboratories visited our lab on January 6, 1965 to review problems relating to stability and handling of sodium-ammonia solutions. They were given a thorough briefing on our experimental techniques as well as of our current work.

2.1 Abstract of Paper Presented at the Pasadena Meeting of the American Physical Society, Division of Fluid Dynamics on November 25, 1964

Dense Gaseous Cold Plasmas*

S. Naiditch

Unified Science Assoc., Inc.

Electronically-conducting gaseous solutions have been produced by dissolving metallic sodium in dense gaseous ammonia, at 130 to 190°C. The solutions are under equilibrium with respect to electronic conductivity, but metastable with respect to chemical stability. Chemical lifetimes of 3000 sec have been obtained. The more dilute gaseous solutions are dark blue in color. A conductivity of 0.7 mho/cm was observed in a sample with an electron density of 7.5×10^{19} electrons per cc, assuming the sodium to be fully ionized. The more concentrated gaseous solutions have a metallic copper-gold reflectivity. In one sample a conductivity of 130 mhos/cm was found, which corresponds to an electron density of 2.6×10^{20} electrons per cc.

*Research work supported by the Office of Naval Research, under Contract NONR 3437(00).

3.0 HALL EFFECT

3.1 INTRODUCTION

Hall effect measurements are frequently used for the determination of the number density and the nature of charge carriers. This effect occurs when an electric current passes the specimen in the presence of a magnetic field. The interaction of the moving charge carriers and the magnetic field B produces an electric field E_H which is perpendicular to both the current density vector and to the magnetic field vector. The measurements can be more easily interpreted if a rectangular sample is used in a magnetic field perpendicular to the direction of the electric current. The Hall field produces a potential difference V_H between the two end surfaces perpendicular to E_H . The Hall voltage V_H is determined by the equation

$$V_H = R_H \cdot I \cdot B \cdot \frac{1}{t} \quad (3.1)$$

I is the specimen current, R is the Hall coefficient, and t is the thickness of the sample. If only one kind of charge carrier is present, the Hall coefficient is given by the equation

$$R_H = \frac{1}{n \cdot e} \quad (3.2)$$

n is the carrier density of the specimen and e is the charge of the carriers. Number density and nature of the charge carrier can be obtained from the modulus and the sign of the Hall coefficient. In the present studies of sodium ammonia solutions, it is planned to determine these important parameters from measurements of the Hall coefficient of the solution.

Hall coefficient measurements of sodium ammonia solutions are complicated by the catalytic effects of metals and the decomposition of the solution. During the previous period of this contract, an electrodeless method for Hall effect measurements was devised. The apparatus utilizes the double a.c. technique^(3.1). Specimen current and magnetic field are a.c. quantities at different frequencies. A frequency of 460 cps is used for the specimen current and the a.c. magnetic field is operated at 60 cps. The Hall voltage is generated at the beat frequencies 400 cps and 520 cps. Measuring one component of the Hall voltage, the 400 cps component in our case, permits the determination of the Hall coefficient. Electrodes for the specimen current are eliminated by inducing the current in a closed loop of glass tubing filled with the substance under test. The Hall voltage is measured by nulling the Hall current and measuring the compensation voltage that reduces the Hall current to zero. The compensation voltage is induced in the closed loop of the Hall voltage detection circuit which consists also of glass tubing filled with the substance under test. The Hall current is detected by an inductively coupled current probe. The devised method eliminates any metal electrodes in contact with the substance whose Hall coefficient is to be measured.

The apparatus was successfully tested by measuring the Hall voltage of a solid state Hall cell. However, the expected Hall coefficients of concentrated sodium ammonia solutions are much smaller than those of materials used for standard solid state Hall cells. If all sodium atoms dissociate into ions and free electrons, one can assume that the Hall coefficient of concentrated sodium ammonia solutions is smaller by a factor 10^{-5} than that of solid state cells. Disturbing effects which are negligible for Hall effect measurements of solid state

materials can be deciding factors for the successful measurements with sodium ammonia solutions. It was assumed that a more thorough test of the apparatus should be performed by measuring the Hall coefficient of mercury. The mercury experiment, the encountered difficulties and the efforts to overcome adverse effects, are the subject of this report.

3.2.0 Experimental

3.2.1 First Attempt at Measuring the Hall Coefficient of Mercury

During the previous period an apparatus was built for the electrodeless measurement of the Hall coefficient of sodium ammonia solutions. A schematic drawing of the apparatus is shown in figure 3.1. As a final test of the apparatus, an attempt was made to measure the Hall coefficient of mercury. For these measurements, it was necessary to calibrate transformers No. 2 and No. 4 of figure 3.1. Transformer No. 2 of figure 3.1 measures the induced specimen current. Transformer No. 4 is used to induce the compensation voltage which nulls the Hall current. The Hall voltage is measured by determining the amplitude of the compensation voltage that nulls the Hall current. A detailed description of the apparatus and the principle of the measurement is given in the report for the period ending 19 August 1964.

Difficulties were encountered in reproducing the calibration after dismantling the transformers. The reason for the different response of the reassembled transformer is the difficulty of reproducing the air gap between the iron cores. This problem was solved by attaching an auxiliary coil of thin wire with the same number of turns to the glass coils No. 2 and No. 4 and calibrating the transformer No. 2 and No. 4 with the auxiliary coils after mounting the Hall cell and the attached glass coil in the apparatus. During the calibration the Hall cell and the glass coils were empty. After calibration of the transformer the cell and glass coils were filled with mercury.

In a separate experiment the accuracy of the described calibration was checked. A single glass coil with an attached auxiliary coil was mounted in a transformer similar to those which are used in the

Hall effect apparatus. Output voltage versus current through the auxiliary coil was measured. Subsequently, the glass coil was filled with mercury and the output voltage versus current through the filled glass coil was measured. Within the accuracy of the meters, the same output voltages were observed for the same currents passing the filled glass coil or the auxiliary coil.

The complicated glass cell including the four coils and the glass tubing for connecting the coils to the Hall cell was filled with mercury. In order to avoid air enclosures which could cause an open circuit, it was necessary to evacuate the cell and the mercury container. After two attempts the cell was filled without air enclosures. The electrical continuity of the exciter current loop and the Hall current loop was checked by inducing a.c. currents in both loops and detecting the current by means of the exciter current and the Hall current detection transformers.

When the a.c. magnetic field was applied to the apparatus a high level of 60 cps pickup noise was observed in the Hall voltage detection circuit. This noise level was higher than that which was observed during the previous experiment with the solid state Hall cell. The reason for the higher pickup noise is the different arrangement of the leads to the Hall cell. In the case of the solid state cell, these leads were closely spaced, thin wires while mercury filled glass tubes were used for connecting the glass Hall cell to the transformers of the Hall voltage detection circuit. These leads could not be spaced as closely as the wire leads of the solid state Hall cell. They enclosed an area A of approximately 6 cm^2 of the pole pieces. From Maxwell's equation

$$\oint \vec{E} \cdot d\vec{l} = - \int \vec{B} \cdot d\vec{S} \approx -B_0 \omega \cdot A \cdot \cos(\omega t) \quad (3.3)$$

one finds for the amplitude of the induced 60 cps voltage a value of 2.2×10^{-2} V if a magnetic field of 1 K gauss is applied. The resistance of the Hall voltage detection loop is approximately 0.1 ohm. The induced 60 cps voltage drives a current of 0.22 amp through the Hall current detection transformer whose approximate sensitivity is 100 mV per 1 mA. A pickup voltage of 22 V can be expected at the output of the Hall current detection transformer. This value is in the same order of magnitude as the observed level of 60 cps pickup noise.

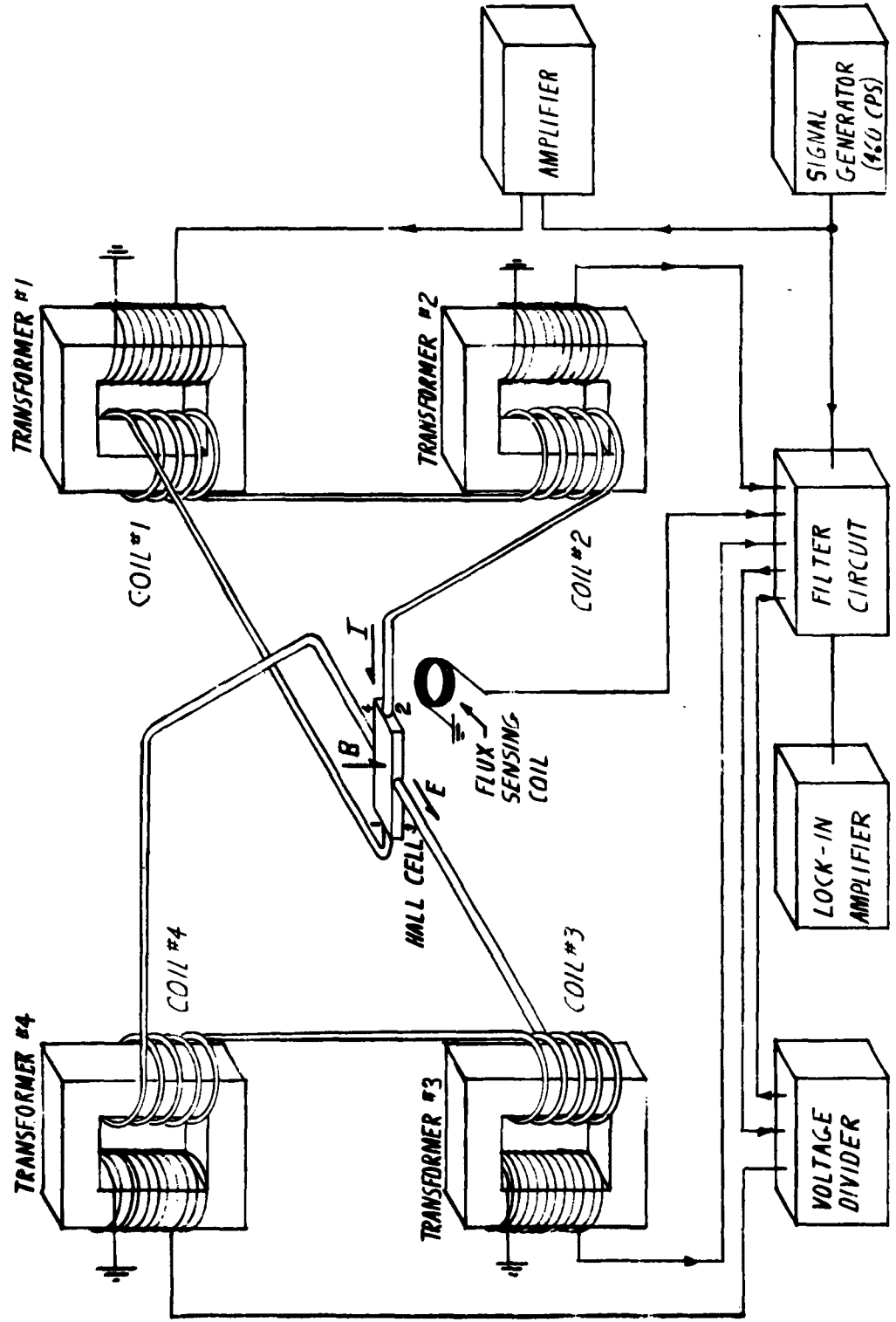
Pickup noise had been taken into account in the design of the apparatus. The output voltage of the Hall current detection transformer passes a filter circuit before it is measured by means of a lock-in amplifier. The commercial band pass filter suppressed the 60 cps components of the pickup noise. However, the higher harmonics of the 60 cps voltage passed the filter circuit and overloaded the lock-in amplifier.

It was not possible to detect the Hall current in the presence of the high noise level. An attempt was made to reduce the pickup noise by means of a bucking coil. 60 cps line voltage and the output voltage of the flux sensing coil which measures the a.c. magnetic field have been used to null the pickup voltage. The amplitude of the compensation voltage was controlled by a voltage divider and a phase shifter was used to adjust the compensation voltage in opposite phase to the 60 cps pickup voltage. The phase relation between pickup voltage and compensation voltage was observed with a dual beam oscilloscope. It was not possible to accurately match

the wave form of the pickup noise which was affected by the non-linearity of the magnet. The 60 cps component of the pickup noise could be nulled but it was not possible to reduce essentially the higher harmonics of the pickup noise. Since the higher harmonics passed the filter circuit unaffected, no improvement of the signal to noise ratio could be achieved by this method.

At this stage in the work, two methods for improving the signal to noise ratio were taken into consideration. One method was aimed at nulling of the higher harmonics of the pickup noise. This approach involves generation of higher harmonics and adjustment of the frequency component in phase and amplitude. Since the noise level of the higher harmonics was larger by a factor of 10^4 than that of the expected signal, it was concluded that the requirement on the stability of phase and amplitude of the compensation voltage would be too high.

It was expected that a more effective reduction of the noise level can be achieved by improving the filter circuit.



HALL CELL AND BLOCK DIAGRAM OF DETECTION CIRCUIT
 FIGURE 3.1

3.2.2 Efforts to Reduce the Noise Level by Improving the Filter Circuit

During the first attempt of measuring the Hall coefficient of mercury, it was observed that the pickup noise which passed the existing filter circuit was predominantly composed of the third harmonic of the 60 cps noise. It was assumed that the pickup noise could be reduced to a sufficiently low level by a high pass filter which suppresses all frequencies below the 400 cps Hall voltage. The output impedance of the Hall current detection transformer is very high and could not be matched by the input impedance of a wave filter without using unusually large components. It was also desirable to achieve the impedance match without loss of the signal voltage. Therefore, a cathode-follower amplifier was chosen for matching the impedances at the Hall current detection transformer and at the wave filter. In order to improve the signal to noise ratio further, the cathode-follower was preceded by an amplifier tuned at the frequency of the Hall voltage.

To prevent intermodulation of the 60 cps noise and the 460 cps unbalanced voltage, negative feedback was used to linearize the characteristic of the amplifier. Figure 3.2 represents the circuit diagram of the active filter.

The design of the passive high-pass filter was based on the image parameter theory^(3.2,3.3). The filter consists of three T-sections. M-derived half sections are added to both ends of the filter. The impedance level of the filter is $R = 1000$ ohms. The cut-off frequency was chosen at 380 cps. For the m-derived half-sections, a factor of $m = 0.57$ was used. The circuit diagram of the filter is shown in figure 3.3.

The new filters were used in connection with the Hall effect apparatus. It was found that the third harmonic of the 60 cps pickup noise was sufficiently suppressed. However, the seventh harmonic of the pickup noise was able to pass the filter circuit without appreciable attenuation and produced a large signal at the output of the signal channel of the lock-in amplifier. As it is indicated in figure 3.1, the lock-in amplifier is used to measure the output voltage of the Hall current detection transformer. The seventh harmonic of the pickup noise is separated by only 20 cps from the 400 cps Hall voltage. Because of this small frequency difference, the tuned signal channel amplifier increased the level of the seventh harmonic. The observed level of the pickup noise was higher by a factor 30 than the expected level of the voltage due to the Hall current. It was not possible to detect Hall current in the presence of this noise level.

An attempt was made to overcome the noise problem by an additional active filter. The frequency of the Hall voltage was changed from 400 cps to 390 cps in order to increase the frequency separation from the seventh harmonic of the 60 cps pickup noise. The frequency change was aimed at lightening the filter problem. The final filter consists of three amplifier stages tuned at 390 cps. The negative feedback of first two stages reduces the amplification factor at resonance frequency to one. The amplification drops very rapidly for signals off the resonance frequency. The gain $g(\omega)$ of a single stage is determined by the equation

$$f(\omega) = \frac{S}{1 + SR_c} \cdot \frac{\omega L}{\sqrt{\left[\frac{1}{Q^2} + \left(\frac{\omega}{\omega_0} \right)^2 - 1 \right]^2}} \quad (3.4)$$

S is the transconductance, L is the inductance of the tank circuit, ω denotes the frequency and ω_0 is the resonance frequency. From equation 3.4 one can see that the bandwidth of the amplifier is reduced by increasing the quality factor Q of the tank circuit. Therefore, high Q components were used to obtain sufficient attenuation at the frequency of the seventh harmonic of the pickup noise. Figure 3.4 represents the circuit diagram of the filter. The tank circuit of the first active filter was also tuned at 390 cps. Figure 3.5 shows the frequency response of the whole filter circuit composed of the first active filter, the high-pass filter and the second active filter.

The filter circuit attenuated the 420 cps component of the pickup noise to a sufficiently low level. However, it was necessary to improve the stability of the circuit by negative feedback from the output of the second active filter to the grid of tube No. 3 in figure 3.4. Because of the relatively high fluctuations which were observed when the filter circuit was used in connection with the Hall effect apparatus, it was decided to build a passive band-pass filter for the attenuation of high frequency components that can cause damped oscillations of the tank circuits used in the second active filter.

The design of the band-pass filter was again based on the image parameter theory. The filter was built for an impedance level of $R = 1000$ ohms. The cut-off frequencies are $f_h = 410$ cps and $f_l = 370$ cps. The filter is composed of two π -sections. The circuit diagram of the filter is shown in figure 3.6. Figure 3.7 represents the frequency response of the filter. The ratio of

output voltage to input voltage V_{in} is expressed in decibels db. These units are defined by the equation

$$db = 20 \cdot \log_{10} \frac{V_{out}}{V_{in}} \quad (3.5)$$

A high attenuation of the 420 cps component has been achieved. However, attenuation in the pass-band could not be avoided because of the low Q factor of the inductors which are used for the circuit. Unfortunately, no better components were commercially available in the required frequency range.

The passive band-pass filter was cascaded with the first active filter, high-pass filter and the second active filter. The fluctuations were essentially reduced, and for the first time, it was possible to use the full sensitivity of the lock-in amplifier for measuring the output voltage of the Hall current detection transformer. Encouraged by this result, all active filters were eliminated by two passive band-pass filters. A transformer was used for matching the impedances of the Hall voltage detection transformer and of the band-pass filter. A low noise Tektronix amplifier was inserted between the band-pass filters to compensate the insertion losses. A step-up transformer followed the first band-pass filter and eliminates the voltage loss of the matching transformer. Figure 3.8 shows a block diagram of the Hall current detection circuit. Relative output voltage for constant input current is plotted as a function of frequency in figure 3.9. The maximum value of the output voltage in figure 3.9 has been normalized to one.

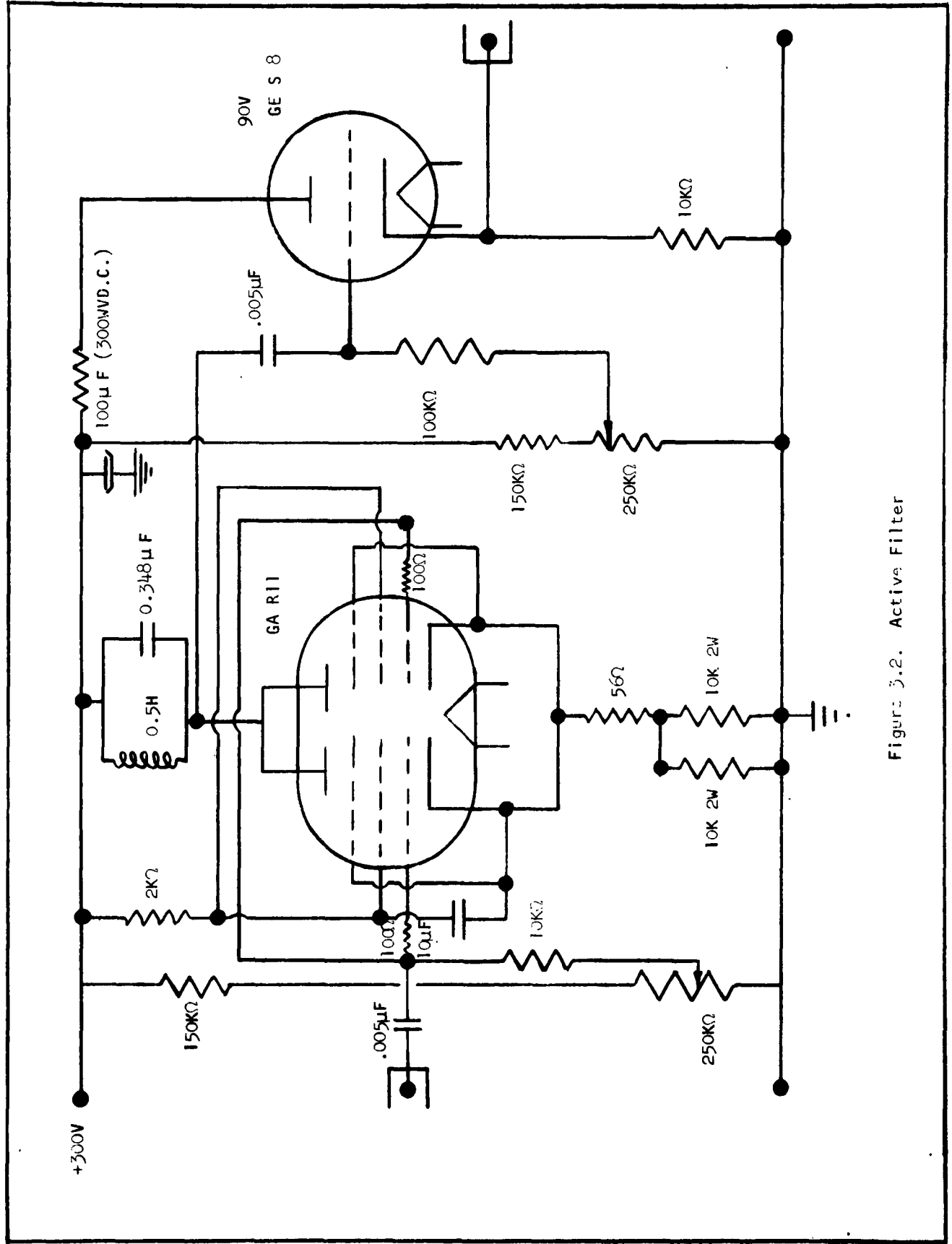


Figure 3.2. Active Filter

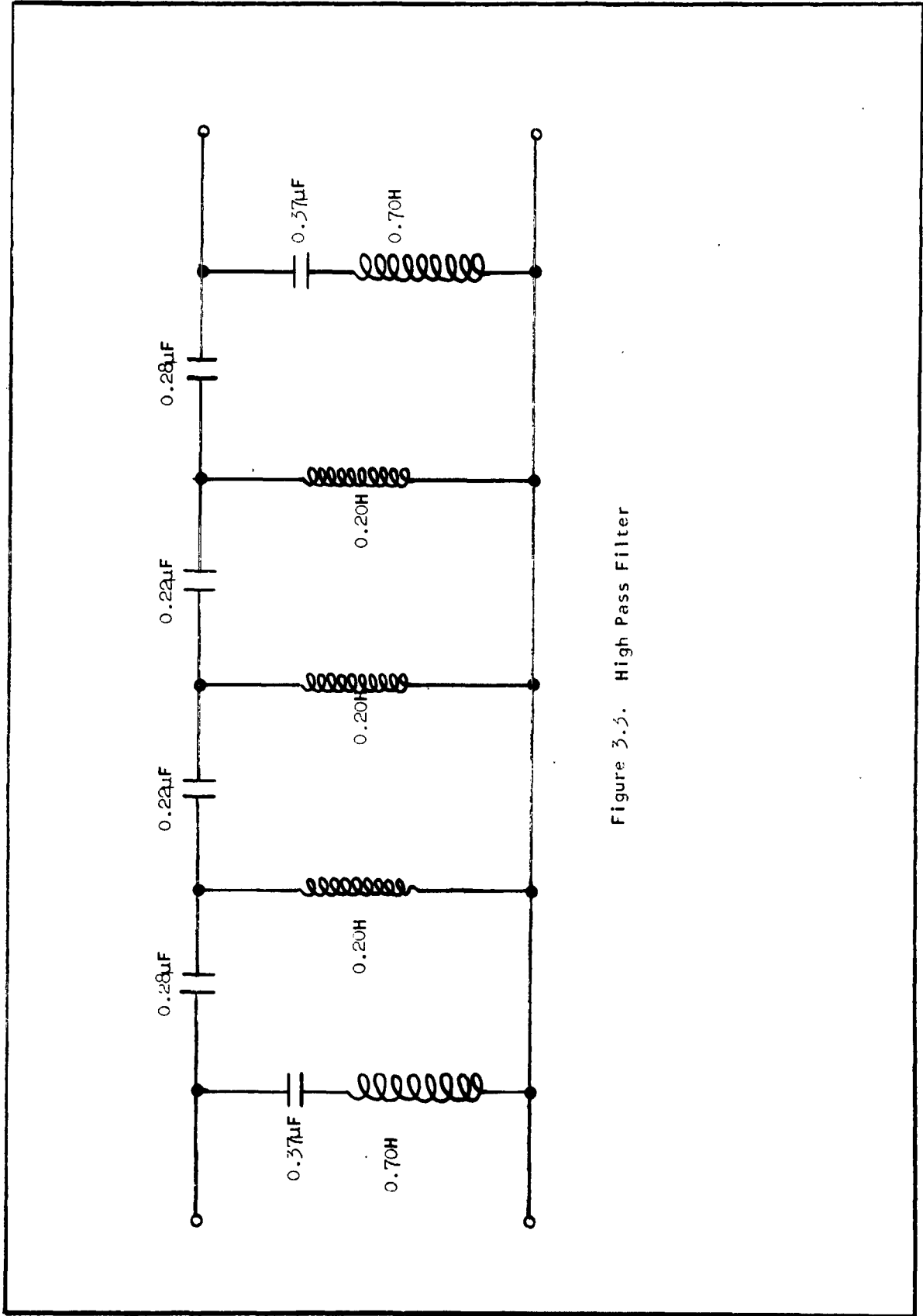


Figure 3.3. High Pass Filter

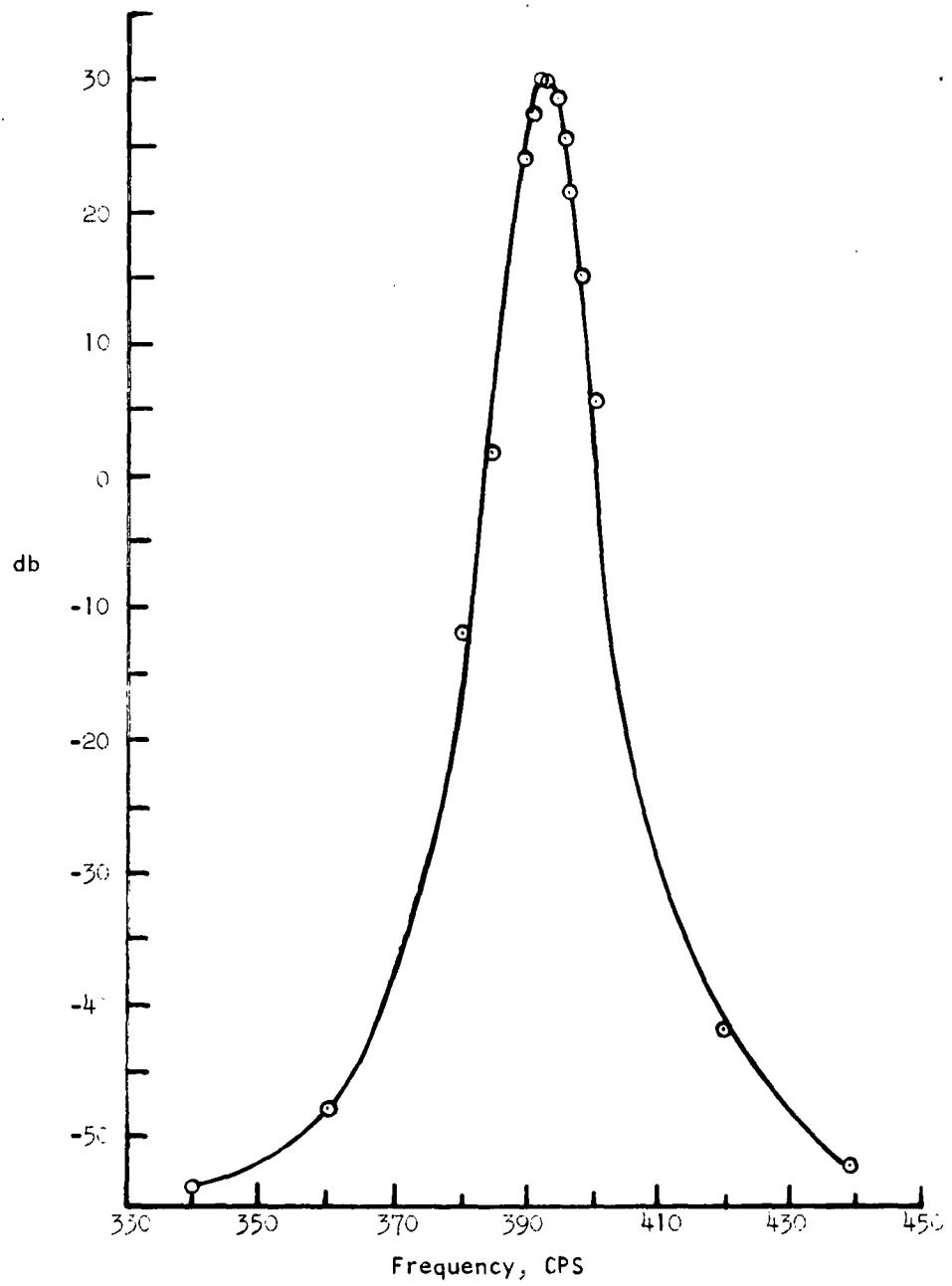


Figure 3.5. Frequency Response of Active and High-Pass Filters

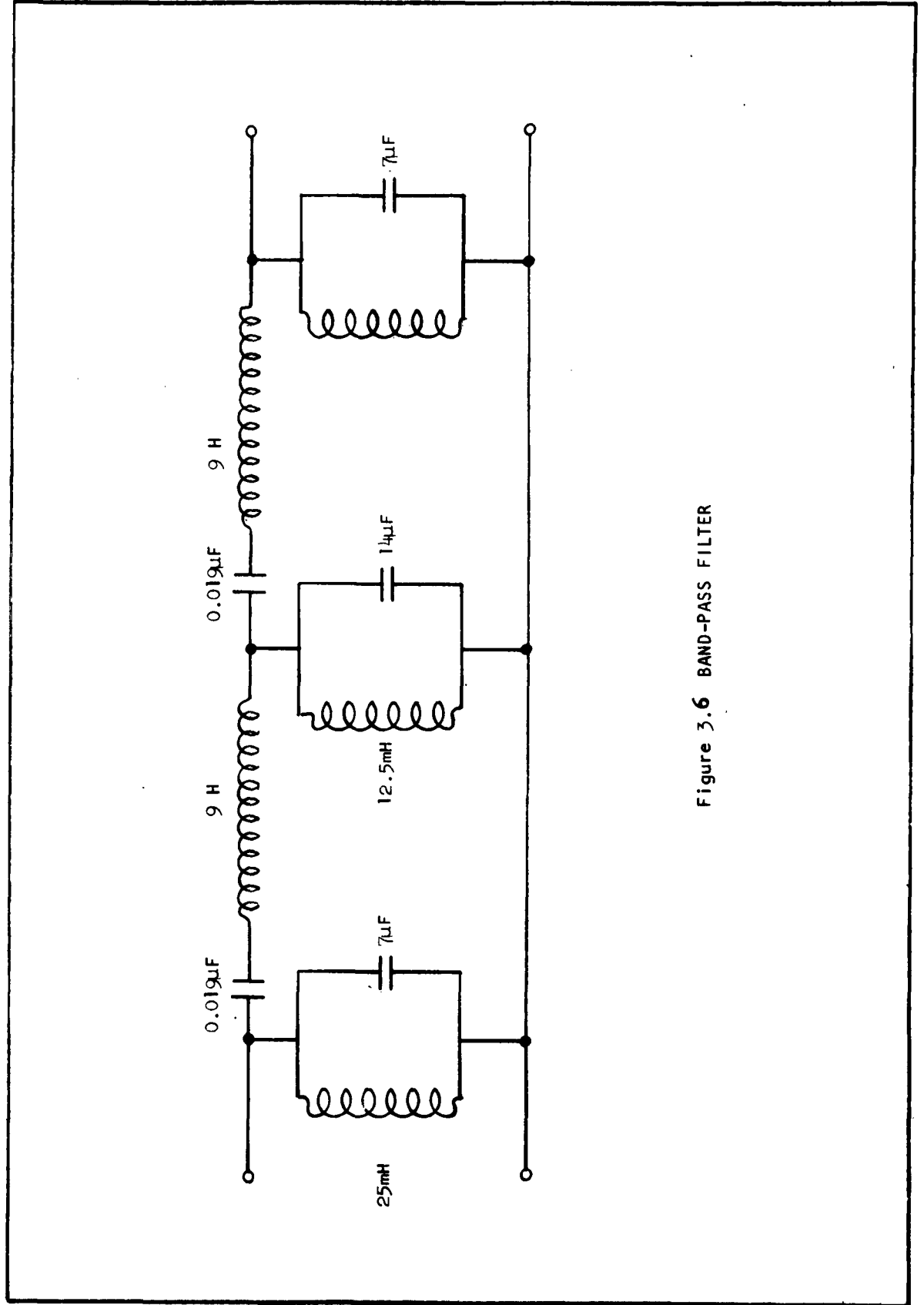
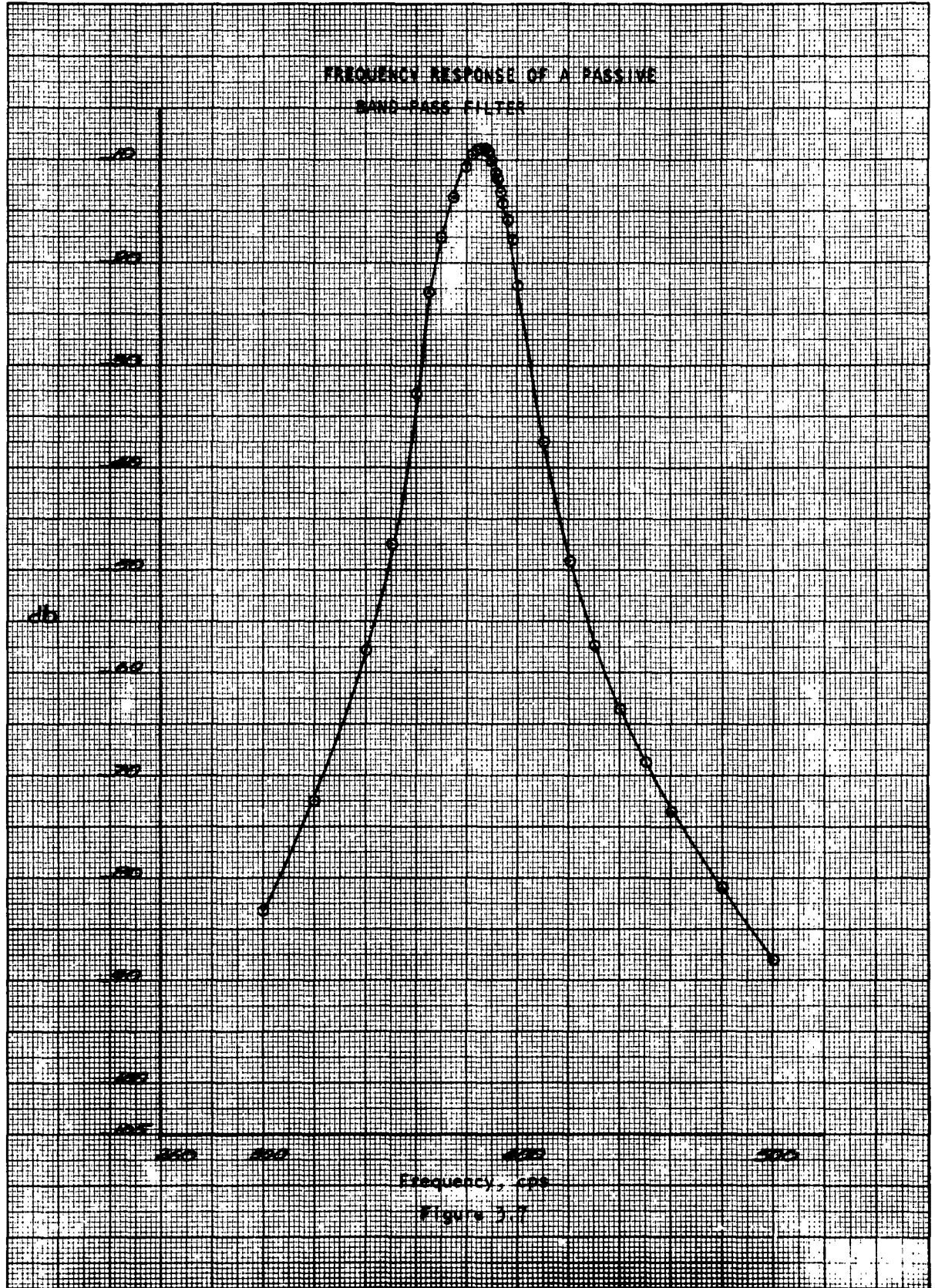


Figure 3.6 BAND-PASS FILTER

K-E 10 X 10 TO THE CENTIMETER 46 1513
1.0 X 25 CM MADE IN U.S.A.
KEUFFEL & ESSER CO



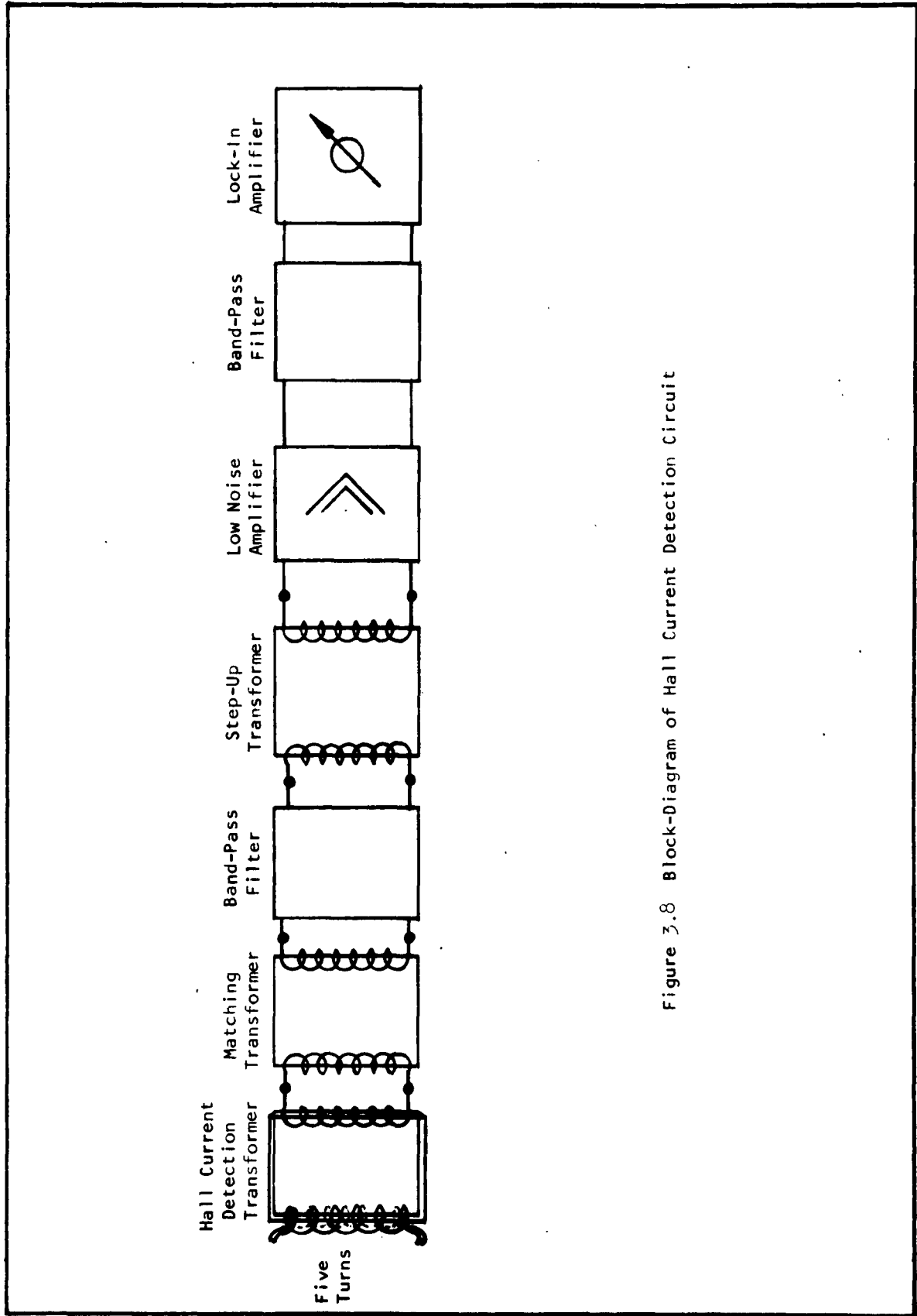
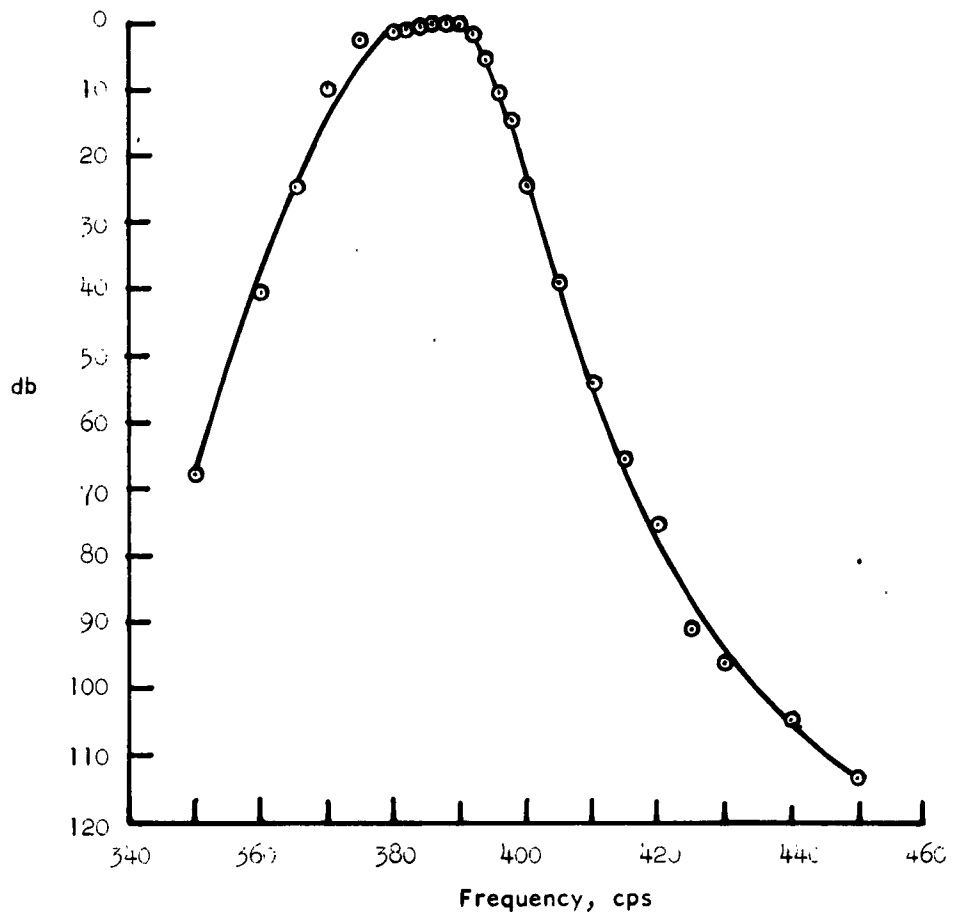


Figure 3.8 Block-Diagram of Hall Current Detection Circuit

Figure 3.9

OUTPUT VOLTAGE FOR CONSTANT INPUT CURRENT
VS
FREQUENCY
(Maximum output voltage is normalized to 1)



3.2.3 Effect of the Improved Filter Circuit on the Noise Level

After the signal to noise ratio had been improved, the experiment to measure the Hall coefficient of mercury was repeated. For the purpose of determining the Hall voltage, an attempt was made to null the observed 390 cps current flowing in the Hall current loop of the apparatus. However, only a small portion of this current could be nulled. Investigation of the amplified output voltage of the Hall current detection circuit revealed a fluctuating 390 cps signal. It was obvious that a current which produced such an output signal could not be nulled by a signal with constant amplitude.

Immediately a test was performed to investigate the cause of the fluctuations. The a.c. magnetic field and the specimen current were shut off. A small 390 cps current of the same value as the expected Hall current was induced in the Hall current loop of the apparatus. The current was detected by the Hall current detection transformer and the subsequent filter circuit including the lock-in amplifier. No fluctuations of the signal amplitude were observed. The experiment proved that the Hall current detection circuit did not generate the distortions.

Since fluctuations of the output voltage of the Hall current detection transformer were found only when the a.c. magnetic field was applied to the apparatus, it was assumed that these distortions are caused by noise in the line voltage which drives the a.c. magnet. From a simplified analysis, a qualitative idea can be obtained as to how a fluctuating sine wave at 390 cps can be generated by impulsive noise at the input of the filter circuit. The Fourier transform of an impulse V_{ξ} with the waveform of a δ -function is a constant.

$$F(V_{\xi}) = A \quad (3.6)$$

The transfer function $\sigma(\omega)$ of an ideal band-pass filter is

$$\sigma(\omega) = \begin{cases} 1 & \text{for } |\omega_1| \leq |\omega| \leq |\omega_2| \\ 0 & \text{for } |\omega_1| > |\omega| > |\omega_2| \end{cases} \quad (3.7)$$

The impulse response $V(t)$ at the output of the band-pass filter is

$$V(t) = \frac{1}{2\pi} \int_{-\infty}^{\infty} F(V_s) \cdot \sigma(\omega) \cdot e^{i\omega t} \cdot d\omega \quad (3.8)$$

Inserting equations (3.6) and (3.7) in equation (3.8) yields

$$V(t) = \frac{1}{2\pi} \int_{-\omega_2}^{-\omega_1} A \cdot e^{i\omega t} \cdot d\omega + \frac{1}{2\pi} \int_{\omega_1}^{\omega_2} A \cdot e^{i\omega t} \cdot d\omega \quad (3.9)$$

$$V(t) = \frac{A}{\pi} \int_{\omega_1}^{\omega_2} \cos(\omega t) \cdot d\omega \quad (3.10)$$

Solving the simple integral of equation (3.10) one gets

$$V(t) = \frac{A}{\pi \cdot t} \left[\sin \omega_2 \cdot t - \sin \omega_1 t \right]$$

The last equation can be also expressed in the form

$$V(t) = \frac{A \cdot (\omega_2 - \omega_1)}{\pi} \cdot \left(\frac{\sin \left\{ \frac{\omega_2 - \omega_1}{2} \cdot t \right\}}{\frac{\omega_2 - \omega_1}{2} \cdot t} \right) \cdot \cos \left(\frac{\omega_2 + \omega_1}{2} \cdot t \right) \quad (3.11)$$

Equation (3.11) shows that the impulse response of a band-pass filter is a decaying sine-wave at the center frequency of the pass-band. If the voltage pulses occur at random at the input of a band-pass filter, the amplitude of the output voltage fluctuates randomly. In the case of the filters used for the Hall current detection circuit, the value

$\omega_2 - \omega_1$ is very small. Therefore, the fluctuations of the output voltage decay slowly. The center frequency of the pass-band is approximately equal to 390 cps. An accurate measurement of the noise frequency is not possible because of the fluctuating amplitude. Qualitatively, the result of this simple analysis agrees with the observed noise at the output of the Hall current detection circuit.

In order to check the assumption that the noise which causes the fluctuating 390 cps sine-wave is generated by distortions of the line voltage, the following experiment was performed. Line voltage was applied over a variable transformer to the input of the filter circuit. The transformer was adjusted for an output voltage equal to the level of the 60 cps pick-up noise. A fluctuating 390 cps sine wave was observed at the output of the filter circuit. The output voltage was similar to the noise which is superimposed to the Hall voltage.

The results of the analysis indicate that the signal to noise ratio at the output of the Hall current detection circuit cannot be improved significantly by additional filters. Since the bandwidth $\omega_2 - \omega_1$ is already small, additional filters would alter the waveform of the distortion without sufficiently reducing the amplitude. However, it is expected that the signal to noise ratio can be improved by filtering the line voltage which drives the a.c. magnet.

3.2.4 Effect of Intermodulation

During the experiments with the Hall effect apparatus, it was observed that for certain adjustments of the gain control on the exciter current amplifier, a large 390 cps signal was generated with only weak magnetic fields. The 60 cps magnetic field was too small to produce a Hall voltage of the observed level. It was assumed that intermodulation of 60 cps voltage and the 450 cps exciter current was the cause of this signal. Since this 390 cps signal cannot be separated from the Hall voltage, it could seriously disturb the measurements. It was further assumed that the 60 cps voltage which is induced in the exciter current loop by the a.c. magnet modulates the 450 cps current. The output stage of the exciter current amplifier is the non-linear element which is needed for the intermodulation.

In order to prove the validity of this assumption, 60 cps signal of the same amplitude as the 60 cps pick up noise was induced in the exciter current loop and specimen current was applied to the apparatus. The magnetic field was shut off. With the Hall current detection transformer and the subsequent filters and amplifiers, it was possible to detect a sizeable 390 cps signal in the Hall current loop of the apparatus.

Intermodulation was reduced to a large extent by using the high pass filter of figure 3.3 between the exciter current amplifier and the exciter current transformer. The filter prevents 60 cps pickup noise induced in the exciter current loop from reaching the amplifier.

To eliminate further distortion of Hall voltage by intermodulation, a twin T 390 cps band rejection filter was added to the circuit. The twin T filter is used between the generator and the amplifier. It prevents the 390 cps signals from entering the amplifier. Finally, the power supply of the amplifier was replaced by batteries. The overall effect of the high-pass filter, the twin T filter and the operation of the exciter current amplifier with batteries was tested by measuring Hall voltages with the filters and without the filters. The same levels of exciter current and of magnetic field were used. A fifteen times larger 390 cps signal was detected by the Hall current detection transformer when the filters were not used.

The line voltage-operated power supply of the amplifier modulated slightly the 450 cps specimen current. The lower side band of the specimen current produced a 390 cps signal in the Hall voltage detection circuit which was 2.5 times as large as the expected Hall voltage.

The lower side band of the modulated exciter current is coupled into the Hall voltage detection circuit by the misalignment of the Hall voltage probes. The unbalanced potential difference between the probes is composed of all frequency components of the specimen current. In the case of a specimen current which is slightly modulated with 60 cps, one of the components is a 390 cps signal which cannot be separated from the Hall voltage by either phase sensitive detectors or filters.

The double a.c. method is described in the literature^(3.1,3.4). However, the possible errors resulting from intermodulation in the

specimen current circuit have not been considered. The errors are negligible for application of the double a.c. method to measurements on precision solid state Hall cells where the misalignment of the Hall probes is small. The errors become significant as soon as the unbalanced voltage is not small in comparison with the Hall voltage. The distortions are not eliminated if a frequency other than 60 cps is used for the magnetic field because the magnetic field always induces a voltage in the specimen current circuit which can modulate the current if both signals pass non-linear elements of the circuit.

3.2.5 Hall Effect Measurements on a Cell with Electrodes

We next tried to measure the Hall coefficient of mercury. A Hall cell with electrodes was used for these measurements. The experiment was primarily aimed at testing the electronic circuit. The Hall voltage measuring circuit was slightly different from that which is shown in figure 3.8. The Hall current detection transformer and the matching transformer were eliminated. The loss in sensitivity was compensated by a tuned amplifier following the low noise amplifier.

An additional alteration of the original apparatus was introduced by measuring the specimen current with a Tektronix current probe. The filtered output voltage of the probe was measured with a vacuum tube voltmeter.

To reduce the noise level in the measuring circuit, we tried to filter the voltage which drives the a.c. magnet. For this purpose, the magnet was operated in a series resonance circuit tuned at 60 cps. The circuit works like a filter for the line voltage. Qualitatively, it was observed that the a.c. magnet produced less noise when it was used in this circuit. The magnet was an improved version of the original design.

Precautions were taken to avoid distortions of the measurements by intermodulation. A twin-T 390 cps band rejection filter was used between the 450 cps generator and the following amplifier. A high pass filter was inserted between the specimen current amplifier and the Hall coil. In spite of these precautions, the first measurements yielded too high values of the Hall voltage. It was

assumed that the results were effected by intermodulation between 450 cps specimen current and 60 cps line voltage. The measurements were repeated. During the second experiment, plate and heater voltage of the specimen current amplifier were supplied by batteries. In order to reduce possible effects of intermodulation further, the amplifier for the specimen current was operated with low gain. Even for maximum magnetic field, the small specimen current reduced the signal level to the limit of the sensitivity which can be obtained with the present Hall voltage detection circuit. The fluctuations superimposed on the Hall voltage were approximately $\pm 20\%$. In order to eliminate the fluctuations, the Hall voltage was observed for a period of 4 minutes. Readings were recorded every 15 seconds. The following results were obtained:

Amplitude of 390 cps component of Hall voltage $V_{390} = 4 \times 10^{-8}$ V

Amplitude of specimen current $I = 0.81$ amp

Amplitude of magnetic field $B = 6.2$ K gauss.

The thickness t of the mercury sample in the glass cell is 0.05 cm.

The evaluation of the measurement was based on the following equation for the Hall coefficient R_H

$$R_H = \frac{2 \cdot V_{390} \cdot t}{I \cdot B} \quad (3.12)$$

A Hall coefficient $R_H = 7.9 \times 10^{-5} \left(\frac{\text{cm}^3}{\text{Amp sec}} \right)$ was found for mercury. The measured Hall coefficient is close to data published in the literature^(3.2).

The main value of the measurement is the accomplishment that it has been possible to reduce errors caused by intermodulation, misalignment and noise to such an extent that the Hall voltage of mercury

can be detected with present apparatus. It should be mentioned that the strong effect produced by intermodulation is due to the difficulty of aligning properly Hall voltage probes of the glass cell. The necessity of a completely enclosed cell imposes difficulties on the fabrication of the cell which otherwise would not exist.

3.3 CONCLUSIONS

The elimination of metallic leads in the electrodeless method of Hall effect measurements caused difficulties on account of the high pick-up noise induced in the circuit consisting of glass tubes filled with the substance under test. The noise level in the Hall voltage detection current could be greatly reduced by passive band-pass filters. Further improvement of the signal to noise ratio can be achieved by filtering the 60 cps voltage for the a.c. magnet.

The experiment with mercury was helpful by indicating the severe errors which can be introduced by intermodulation if the alignment error of the Hall voltage electrodes cannot be sufficiently reduced. It has been possible to eliminate the intermodulation in the circuit of the specimen current to such an extent that the Hall coefficient of mercury could be measured in a cell with electrodes.

3.4 PROGRAM FOR THE NEXT PERIOD

The work during the next period will be concentrated on measurements of the Hall coefficient of sodium ammonia solutions. The construction of a new apparatus will be completed and an environmental chamber will be built to control the temperature of the sodium ammonia solution during the measurements.

Efforts to improve the signal to noise ratio will be continued. It is planned to filter the 60 cps voltage for the a.c. magnet.

Intermodulation will be reduced further by an improved wave filter in the specimen current circuit. It is also planned to improve the construction of the glass Hall cell to reduce the alignment error.

3.5 REFERENCES

- 3.1 Rev. Scientific Instr. 21, 1028 (1950).
- 3.2 Gordon Newstead, General Circuit Theory, John Wiley and Sons, Ltd., 1959.
- 3.3 Richard Feldtkeller, Einfuehrung in die Siebschaltungstheorie, S. Hirzel Verlag Stuttgart, 1950.
- 3.4 Physical Review, 135, A1589, 1964.

4.0 MAGNETIC SUSCEPTIBILITY

4.1 Introduction

The polarizability of matter by magnetic fields is described in terms of the magnetic susceptibility. This quantity is defined by the equation

$$M = K \cdot H$$

where M is the magnetic moment per unit volume of the substance and H is the magnetic field strength. The polarization of matter results from the interaction of the magnetic field with the electronic structure of the atoms. The effect of the magnetic field on the electron orbits produces a magnetic moment which is oriented opposite to the applied field. The diamagnetic properties of matter are determined by this form of interaction. Orientation polarization occurs in substances whose constituent atoms have an electronic structure with an overall magnetic moment. An applied magnetic field tends to orient these magnetic moments and produces thus a macroscopic magnetic moment of the substance. The paramagnetic properties of matter are due to the orientation polarization. Since thermal agitation within the matter counteracts the orientation of atomic magnetic moment, the paramagnetism is strongly temperature dependent.

Measurements of magnetic susceptibility have been used to test models for the electronic structure of various substances. The work planned under this contract includes measurements of magnetic susceptibilities of sodium ammonia solutions. The magnetic susceptibility of these solutions for various concentrations of sodium and for various temperatures is important for the understanding of the electron states in the solution.

Previous investigation of the susceptibility of sodium ammonia solutions has been conducted by Huster^(4.1) and Thode^(4.2). Huster measured the susceptibility for mole ratios between 1.68×10^{-5} and 1.51×10^{-1} . He observed decreasing atomic susceptibility with increasing mole ratio.

Atomic susceptibility is defined as the susceptibility per gram atom. The dependence of the atomic susceptibility on the concentration was explained by the model of a free electron gas. The low values of atomic susceptibility at high concentration and low temperatures are attributed to the degenerate energy distribution of the electron gas which means pairing of the spins for most of the electrons except for those at the highest energy levels. The observed magnetic susceptibilities were below the theoretical value for a degenerate gas but above the value which is obtained when random diamagnetism is taken into account.

Thode investigated the temperature dependence of the magnetic susceptibility for extremely dilute solutions at 230°K and 206.8°K. He found that qualitatively the paramagnetic electron gas followed Curie's law.

The planned investigations are aimed at supplementing the existing data by extending the temperature range of the measurements. Magnetic susceptibilities of both liquid and gaseous sodium ammonia solutions will be measured at temperatures from -50 to +150°C.

4.2 Experimental

4.2.1 Design of the Apparatus

Of the different ways of measuring magnetic susceptibilities, the Gouy method was chosen for the studies of sodium ammonia solutions. This method measures the force which a magnetic field exerts on a specimen. The sample container and the pole piece configuration of the apparatus are shown in fig. 4.1. The magnetic field is horizontal and exerts a vertical force on the sample which is measured by an analytical balance.

The sample has a uniform cross section and extends from a region of strong uniform magnetic field H to a region of small field H_2 above the pole pieces. The total force F on the sample is determined by the

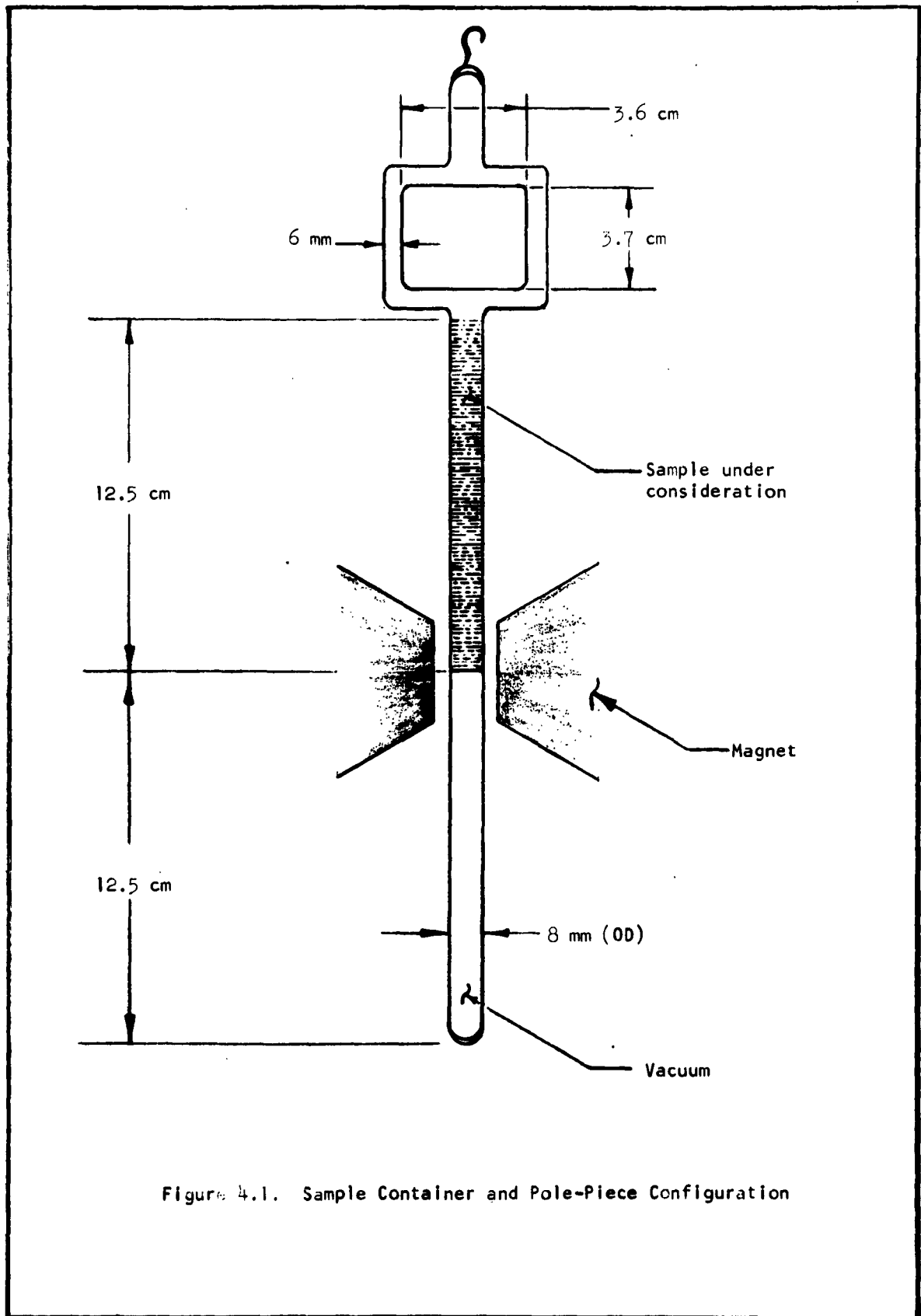


Figure 4.1. Sample Container and Pole-Piece Configuration

equation

$$F = \frac{1}{2} (K_1 - K_2) \cdot A \cdot (H_1^2 - H_2^2) \quad (4.1)$$

K_1 is the volume susceptibility of the specimen. K_2 is the susceptibility of the medium in the lower compartment of the sample tube. Since this part of the tube is evacuated, K_2 is zero.

H_2 is negligible because the designed sample container extends far enough above the pole pieces. Equation (4.1) can be re-written in the simplified form

$$F = \frac{1}{2} K_1 \cdot A \cdot H_1^2 \quad (4.2)$$

The planned work on magnetic susceptibility of sodium ammonia solutions is aimed at measurements at elevated temperatures. Therefore, it was necessary to design a magnet whose windings can withstand temperatures up to 200°C. The design of the magnet was based on a balance sensitivity of 0.05 mg. The magnetic field should be sufficiently strong to exert a measurable force on the specimen. The expected values for the magnetic susceptibility are in the order of 10^{-7} (c.g.s. units). Assuming a magnetic field of 6000 oersteds, one finds a force of 0.5 mg from eq. 4.2 which can be measured with the balance.

The estimate of the necessary number of ampere turns $n \cdot l$ for the electromagnet was based on the equation

$$n \cdot l = B_a + A_a \cdot \left[\frac{l_a}{\mu_0 \cdot A_a} + \frac{l_m}{\mu \cdot A_m} \right] \quad (4.3)$$

A_a and A_m are the cross section areas of the magnetic flux in the gap and in the iron yoke, respectively. l_a and l_m are the corresponding path lengths, in air and in the iron. The evaluation of eq. 4.3 yielded a value $n \cdot l = 7200$ ampere turns for a magnetic field of 6000 gauss. Coils for 7200 ampere turns have been constructed.

In order to relate the observed susceptibility to the correct concentration of the sodium, it is necessary to measure concentration as well as susceptibility of the same sample. The sample cell is designed to facilitate measurements of the concentration. The upper part of the sample cell in fig. 4.1 is shaped as a torus and can be filled with the solution under test by inverting the cell. The dimensions were chosen such that the torus is completely filled when the cell is inverted. The filled torus represents a closed circuit and concentration measurements can be performed by measuring the electrical conductivity of the solution by inductive method.

4.2.2 Measurements of Magnetic Susceptibility

The electro magnet of the apparatus was calibrated by measuring the magnetic field vs current. A standard solid state Hall cell was used to measure the magnetic field. The field was found to vary linearly with current. The measurements were repeated with reversed current. However, no noticeable effect of hysteresis was found. The iron core of the magnet is made of laminated silicon steel. A plot of magnetic field vs current is shown in fig. 4.2.

The Gouy method of measuring the magnetic susceptibility requires a homogeneous magnetic field. For this reason, the spatial variation of the magnetic field was measured in the X (vertical) and Y (horizontal) directions assuming the origin in the center of the gap and the magnetic field in the Z (horizontal) direction. Plots of magnetic field vs distance from the center of the gap are shown in fig. 4.3 and fig. 4.4. From these plots, one can see that a sufficiently large area of homogeneous field is available to perform measurements according to the Gouy method.

In a first experiment an attempt was made to determine whether the sensitivity of the apparatus is sufficient to detect the force which the magnetic field exerts on the sample. For this purpose, an aluminum rod was suspended from the hook of a balance so that its lower end is in the center of the field and its upper end beyond the influence of the field. It was observed that the force was detectable but the surrounding air had considerable effect on the measurements. In order to avoid disturbing effects on following measurements, a plastic shield was added to the apparatus. The shield protects the sample and the suspension wire from effects of moving air.

In a following test of the apparatus, we attempted to measure the magnetic susceptibility of distilled water. The value of the susceptibility of this material is well known. The upper half of the sample tube which is shown in fig. 4.1 was filled with water. The force on the sample due to the magnetic field was measured. Fig. 4.5 shows a plot of the force vs the square of the magnetic field. As can be expected from eq. 4.2 the measurements follow a straight line. The evaluation of the measurements yielded a value of $\chi_w = -0.70 \times 10^{-6}$ (c.g.s. units) for the susceptibility of distilled water.

The known value of the literature is

$$\chi_{\text{water}} = -0.72 \times 10^{-6} \text{ (c.g.s. units)}$$

The measured value differs by 3% from that of the literature.

The susceptibility of liquid ammonia was measured at room temperature. The measurements are plotted in fig. 4.6. The mean value of the measured susceptibility is

$$\chi_{\text{NH}_3} = -0.90 \times 10^{-6} \text{ (c.g.s. units)}$$

The root mean square error of the measurements was 4.75%.

At room temperature, the values for the susceptibility of ammonia are not available. At -75°C and -35°C , Huster found for the susceptibility of ammonia the value $-0.9600 \cdot 10^{-6}$ and $-0.9667 \cdot 10^{-6}$ (c.g.s.), respectively.

The magnetic susceptibility of two samples of sodium ammonia solutions with different mole ratios were measured at room temperature. The observed volume susceptibilities were -0.172×10^{-6} (c.g.s. units) and -0.118×10^{-6} (c.g.s. units) for the mole ratios 15.61×10^{-2} and 17.92×10^{-2} , respectively. The relative root mean square error was approximately 3%.

Based on Kikuchi's^(4.4) density measurements, the volume susceptibilities were converted to mass susceptibility of the solutions. The molar susceptibility x_a of sodium in ammonia was calculated using Wiedemann's mixing rule^(4.1) of eq. (4.4).

$$x_a = r_1 \cdot [x_{\text{sol}} (17.03 + 23.00 r_2) - x_{\text{NH}_3} \cdot 17.03] \quad (4.4)$$

x_{sol} and x_{NH_3} are the mass susceptibilities of the solution and ammonia, respectively. r_1 is the ratio of moles of ammonia to moles of sodium. r_2 is the reciprocal value of r_1 .

The reduction of the volume susceptibilities to molar susceptibilities yielded the following results

$$x_a = +58 \cdot 10^{-6} \text{ [cgs] for } r_2 = 15.6 \cdot 10^{-2}$$

and

$$x_a = +61 \cdot 10^{-6} \text{ [cgs] for } r_2 = 17.9 \cdot 10^{-2}$$

Figure 4.2. Calibration Curve of Electromagnet

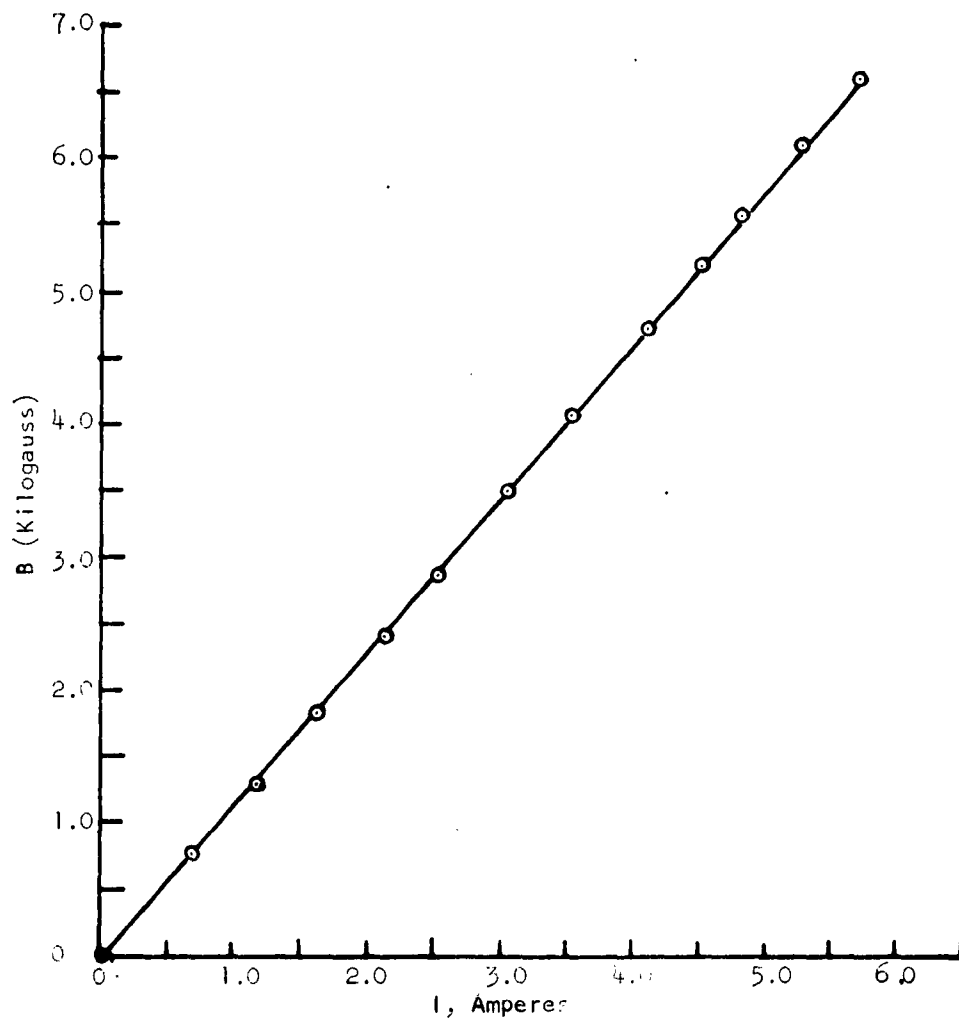


Figure 4.3. Spatial Variation of Magnetic Field
In the X-Direction

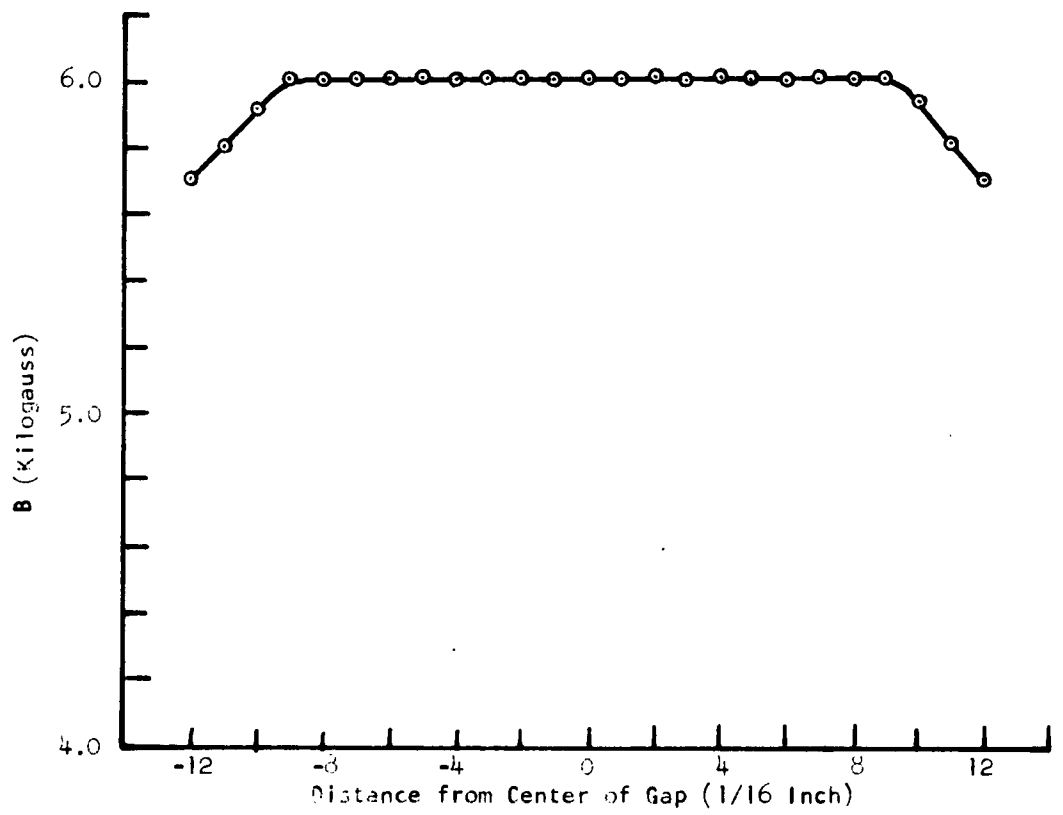


Figure 4.4. Spatial Variation of Magnetic Field in y-Direction

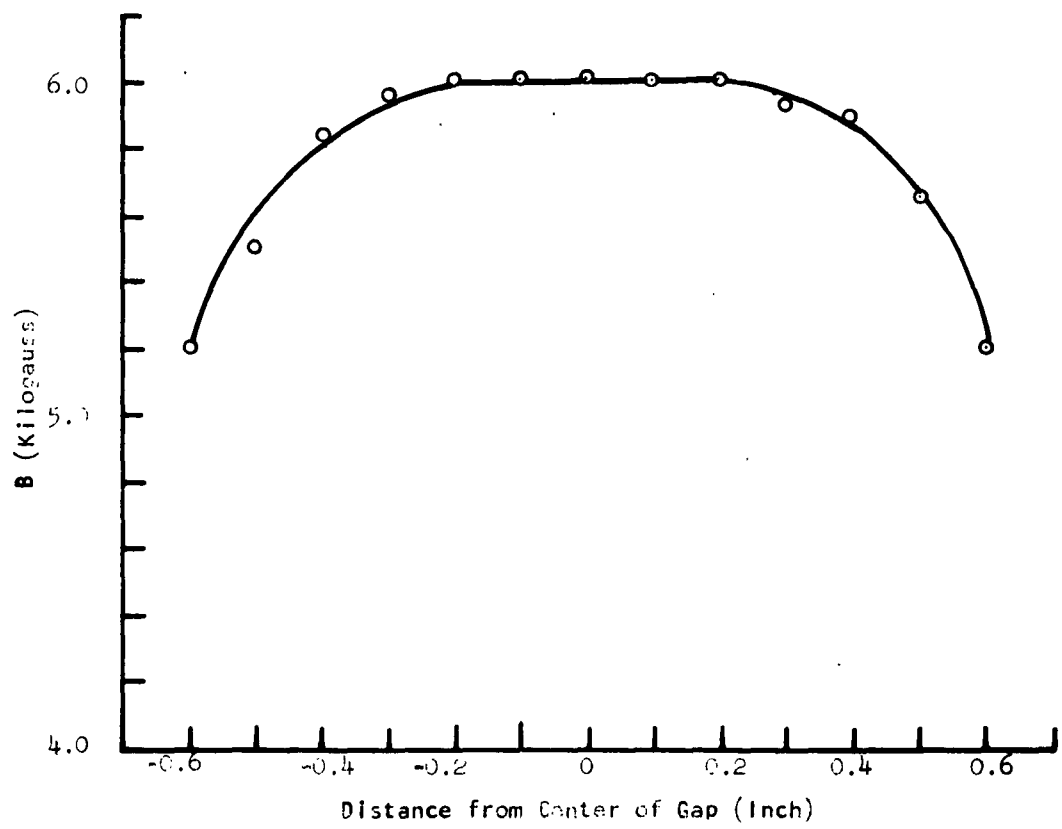


Figure 4.5. Force vs Square of Magnetic Field
(Distilled Water)

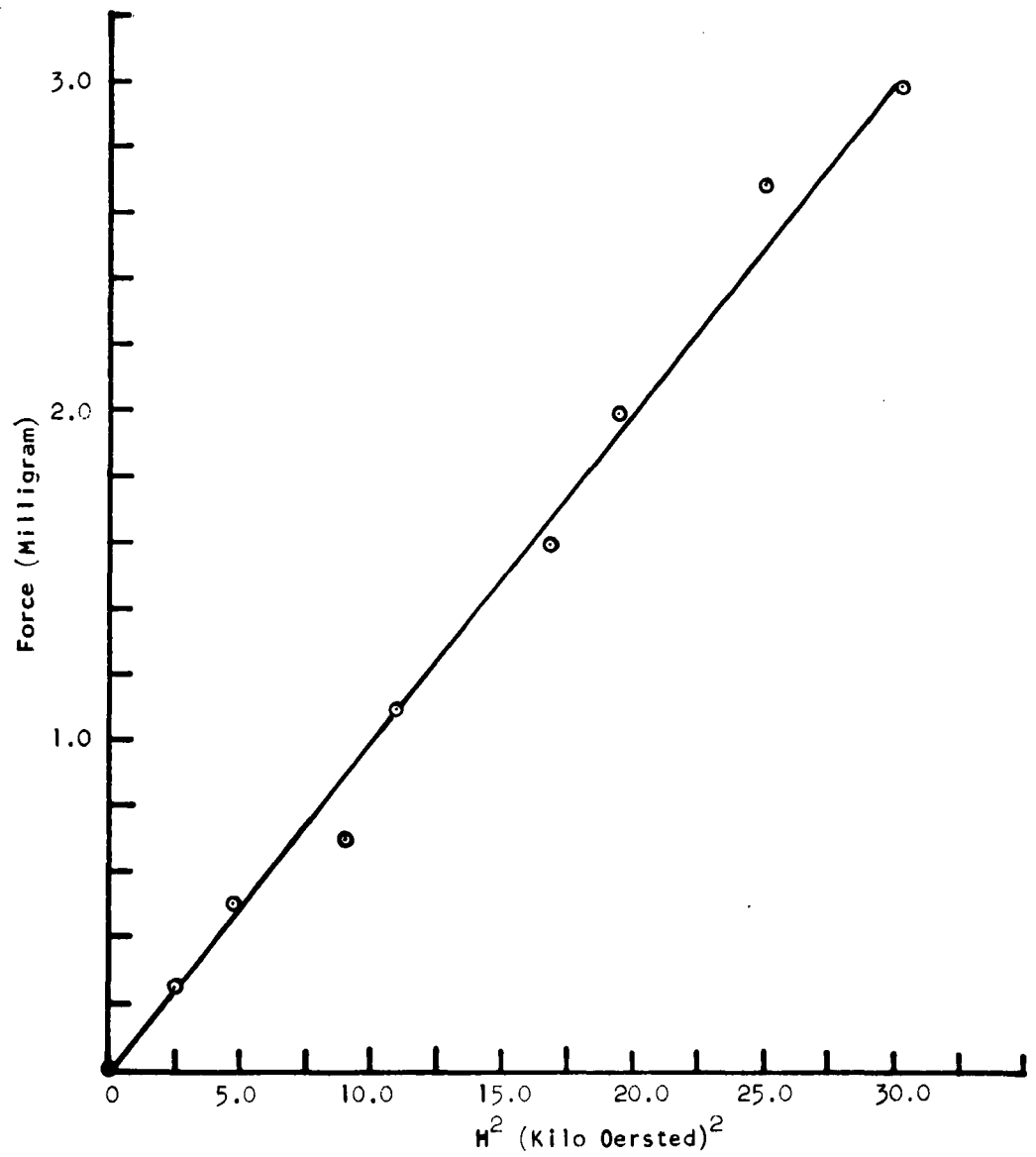
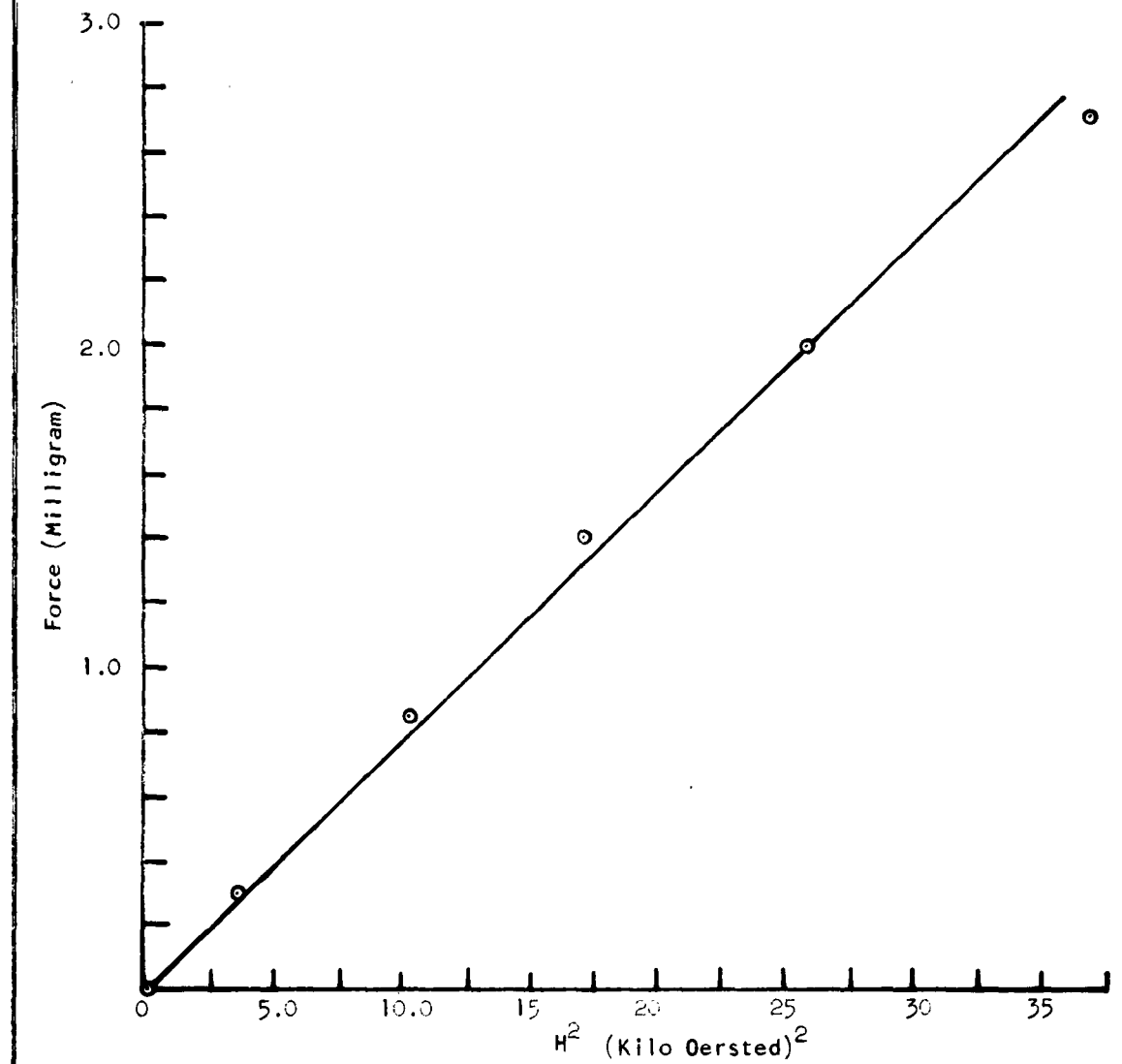


Figure 4.6. Force vs Square of Magnetic Field
(Measured for Ammonia)



4.3 Conclusions

The measurements of magnetic susceptibilities performed at room temperature were primarily aimed at testing the apparatus. The plotted values of force vs the square of the magnetic field in figs. 4.5 and 4.6 follow the correct force law of eq. 4.2. These results prove that the correct effect was measured and disturbing effects were sufficiently reduced. The measured susceptibility of distilled water could be compared with known values of the literature and agreement was found within the accuracy of the measurement.

4.4 Program for the Next Period

An environmental chamber for magnetic susceptibility measurements at elevated temperatures will be constructed. A search coil connected to a ballistic galvanometer will be calibrated for magnetic field measurements above room temperature. As soon as the environmental chamber is operational, measurements of magnetic susceptibilities vs temperature will be performed with sodium ammonia solutions of different concentrations.

4.5 References

- 4.5.1 E. Huster, Ann. Physik 33, 477 (1938).
- 4.5.2 H. A. Thode, Dissertation, University of Chicago, 1940.
- 4.5.3 Electricity and Magnetism by B. I. Bleaney and B. Bleaney.
- 4.5.4 S. Kikuchi, J. Soc. Chem. Ind., Japan, 47, 488 (1944).

5.0 RESEARCH ON SURFACE CONTAMINANTS AND SOLVENT PURITY

5.1 Introduction

The study of the effect of surface contamination on the decomposition of sodium-ammonia solutions has been extended. The procedure is that introduced by Warshawsky^(5.1) and was described in a previous report^(5.2). The experimental system is shown in figure 5.1.

Briefly, the experimental procedure consists of cleaning a pyrex test tube, sealing it onto a vacuum system, then baking out at high vacuum. A small glass-enclosed iron rod with a thin sodium film on its surface is transported to the bottom of the tube. Ammonia is subsequently brought in as a vapor and condensed onto the sodium at liquid nitrogen temperature. The solution is then thawed and held at -78°C for 15 minutes after which the ammonia is distilled into another tube to prevent trapping of hydrogen. The hydrogen evolved during this period from reaction with the surface is measured using a combination Toepler pump-McLeod gauge.

In a previous report, data are given for the amount of contaminant left by various cleaning procedures. Of all the cleaners used, a combination of 33% HNO_3 , 5% HF, 2% Alconox and 60% water has been shown to leave the least amount of residue which reacts with the sodium-ammonia solutions. This is known as "HF Cleaner". It has been proposed as a good cleaner for glass and silica by Crawley^(5.3).

Present tests are aimed at determining the effects of the HF cleaner ingredients; the effects of rinses following the HF cleaner; the effect of a final rinse with anhydrous ammonia; the effect of bakeout conditions; the effect of added contaminants; the effectiveness of various solvent purifications; and the effects of a seal-off under vacuum.

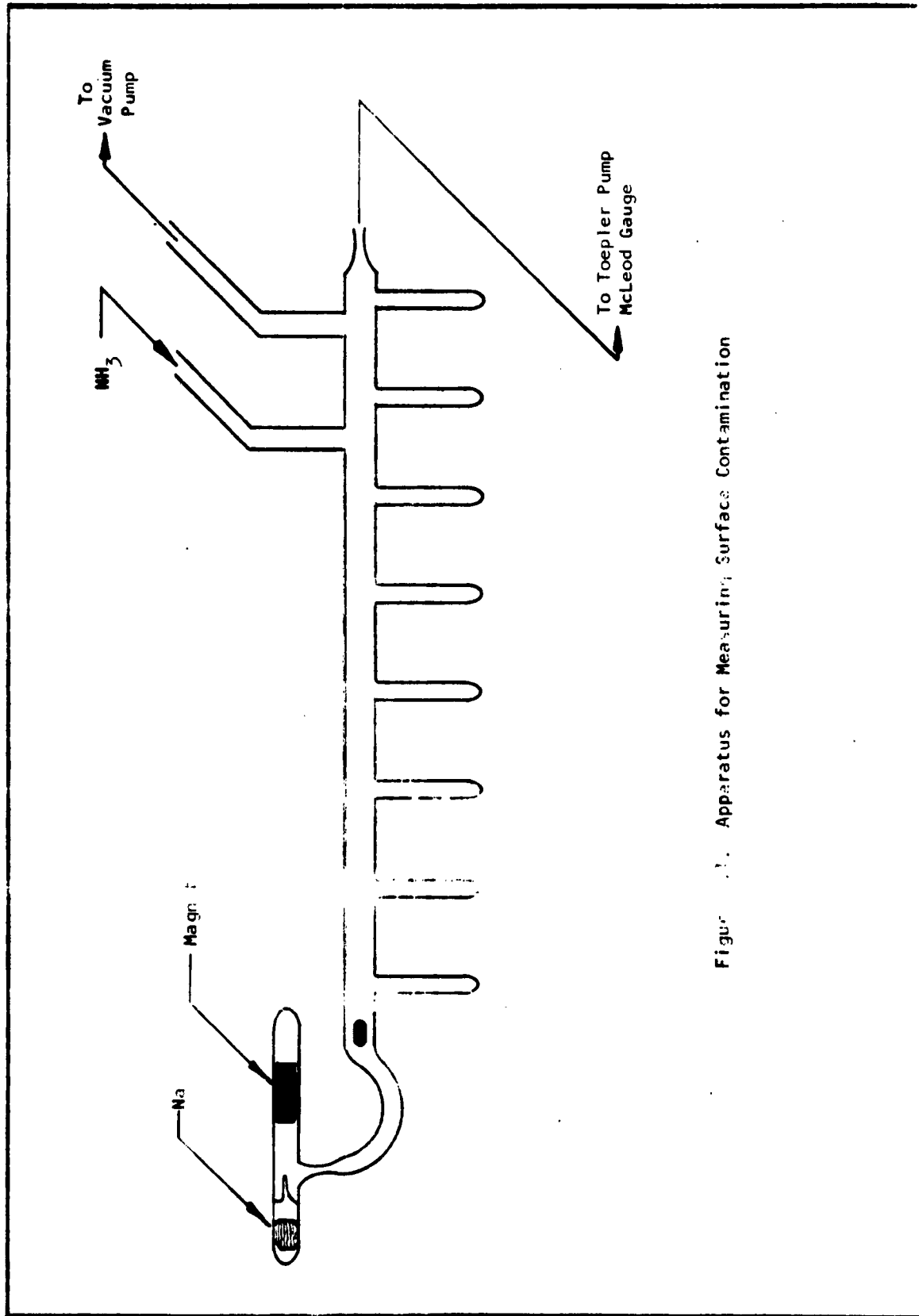


Figure 1. Apparatus for Measuring Surface Contamination

5.2 Experimental Results

5.2.1 Elimination of Surface Contamination

In order to determine what makes the HF cleaner a superior one for our purposes, studies were conducted on the contaminants left by the specific ingredients as well as a solution of the above mentioned composition. The results in Table 5.1 show that contaminants are far more efficiently removed by the cleaner than any of the three components used individually. HF in particular left a large amount of contaminants comparable to the results obtained without cleaning.

TABLE 5.1

EFFECTS OF HF CLEANER INGREDIENTS

Pyrex tubes baked under vacuum for two hours at 400°C, then for one hour at 200°C.

	<u>Wash</u>	<u>Molecules</u> <u>H₂O/sq. Å</u>
The effects of various washes followed by a water rinse.	5% HF	62, 64*
	Conc. HNO ₃	24
	Soap and Water	5,2
	HF Cleaner	2.2
The effects of various washes followed by rinses with aqua regia, then H ₂ O	None	3.2
	5% HF	3.7
	HF Cleaner	0.4 ± 0.2

*The 62 value is without rinse and the 64 value without bakeout.

Since examination of the results in table 5.1 indicated variations due to the rinse following the HF cleaner, a study was conducted to determine the best rinsing procedure for this particular wash. It

is seen in table 5.2 that a rinse with aqua regia followed by several water rinses was the most effective one. The aqua regia, water rinses appear to remove contaminants left by the cleaner. The combination of an HF cleaner wash followed by an aqua regia rinse and six distilled water rinses is now our standard cleaning procedure.

TABLE 5.2

EFFECT OF RINSES FOLLOWING WASHING WITH HF CLEANER

All samples were washed with the HF cleaner, rinsed sequentially with the solvents indicated, then sealed onto the system and baked under vacuum at 400°C for two hours and at 200°C for one hour. The number of rinses with each solvent is indicated in parentheses after the solvent.

<u>Rinse</u>	<u>Molecules H₂O/sq. Å</u>
Aqua Regia (1); Alcohol (2)	6.8
H ₂ O (6); Trichlorethylene (1)	4.9
Chromic Acid (1); H ₂ O (6)	2.6
H ₂ O (6)	2.2
HNO ₃ (1); H ₂ O (6)	1.9
H ₂ O (6); NH ₄ OH (1)	1.6
Aqua Regia (1); H ₂ O (6); NH ₄ OH (1)	1.4
H ₂ O (6); Alcohol (1)	1.3
Aqua Regia (1); H ₂ O (6)	0.4 ± 0.2

Another possible rinse is that with anhydrous ammonia. Final rinsing under vacuum with anhydrous ammonia has been reported to be more effective in dehydrating halides than baking in vacuo. Therefore, this method was evaluated to measure its effectiveness in eliminating or removing surface water. The results are summarized in table 5.3

and show that rinsing with ammonia is indeed effective in decreasing the surface water on glass. However, no improvement has been obtained by rinsing with ammonia when the glass has been cleaned with our standard procedure of HF cleaner followed by aqua regia and water rinses. An increased amount of contaminants was observed if the rinsing ammonia was not of the highest purity. The impurities found after various purifications of ammonia are discussed in section 5.2.2.

TABLE 5.3
EFFECT OF FINAL RINSING WITH
ANHYDROUS NH_3 AFTER EVACUATION

All pyrex glass tubes baked in vacuo at 400°C for two hours, then at 200°C for one hour. All results are obtained with purified NH_3 for the reaction with the sodium.

<u>Wash</u>	<u>Rinse</u>	No <u>NH_3 Rinse</u>	Molecules $\text{H}_2\text{O}/\text{sq. } \text{Å}$		
			Purified <u>NH_3 Rinse</u>	Tank <u>NH_3 Rinse</u>	Dried <u>NH_3 Rinse</u>
HNO_3	H_2O	24	11	--	--
NaOH	H_2O	4.3	2.2	--	--
HF Cleaner	Aqua Regia; H_2O	0.4 ± 0.2	0.4	3 ± 1	0.3

In addition to the studies of chemical cleaning of the glass surfaces, further investigations were conducted on the effect of bakeout in vacuo. The experiments were aimed at reducing the contaminants with a minimum of bakeout time. The results are summarized in table 5.4. Bakeout removes water from surfaces with high water content. Only a slight improvement in the reduction of the water content was obtained when the more effective chemical cleaners were used prior to baking of the glass. Increased bakeout temperatures above 400°C did not

further reduce the contaminants if the HF cleaner was used. In one experiment, the bakeout temperature was accidentally raised beyond 550°C for a period of one hour. The pyrex tubes almost completely collapsed but no further reduction of contaminants was noted. Experiments with prolonged bakeout time which were proposed by Warshawsky^(5.1) resulted in only slightly less surface water.

TABLE 5.4
EFFECTS OF BAKEOUT

Wash	Rinse	No Bake	Molecules H ₂ O/sq. Å		
			400° Bake (2 hrs. 400° 1 hr. 200°)	500° Bake (2 hrs. 500° 1 hr. 200°)	400° Bake 200 Hrs.
None	None	59	78	--	--
HNO ₃	H ₂ O, Acetone	20	11	--	--
HNO ₃	H ₂ O, NH ₄ OH	14	4.4	--	--
Aqua Regia	H ₂ O	7	7	--	--
Hot Soap and water	H ₂ O	5.2	4.2	--	--
Hot Aqua Regia	Hot H ₂ O	2.9, 6.0	3.2	--	--
HF Cleaner	Chromic Acid, H ₂ O	--	2.6	2.3	--
HF Cleaner	H ₂ O	2.2	2.2	--	--
HF Cleaner	Aqua Regia, H ₂ O	--	0.4 ± 0.2	0.5 ± 0.1	0.26 ± 0.03

5.2.2 Effectiveness of Ammonia Purification

After investigating methods of reducing water content on the container walls, the effectiveness of ammonia purification techniques was studied. Ammonia was removed at four different stages of the presently used purification train and tested for water content. The four stages gave us four different grades of purity. The first grade of purity is Matheson tank ammonia which is 99.99% anhydrous ammonia. The second grade was obtained by passing tank ammonia through activated charcoal in a baked vacuum system. For further reduction of the water content, the filtered ammonia is stored on sodium in the vacuum system at -78°C overnight. This procedure yields the third grade of ammonia. The final, or fourth, grade results from further purification by vacuum fractionation.

Since the ammonia samples were stored in a stainless steel transfer tank prior to testing, the purer grades of ammonia could have become contaminated by the absorbed water from the tank wall. The tank was not bakeable so that sorbed water was undoubtedly present. The contaminants found in the final grade of ammonia may have been introduced by the transfer tank.

The amount of contaminants is measured by the evolved hydrogen. By repeating the measurements with the same sample of ammonia in tubes cleaned by previous reaction with sodium ammonia solution, the amount of evolved hydrogen is reduced to 1×10^{-9} moles per milliliter of ammonia. Cleaned surfaces which had been treated with high purity sodium-ammonia solutions cannot contribute to evolution of hydrogen beyond this amount. In this series of measurements, all glass sample containers were cleaned and treated with sodium-ammonia

solution prior to measurement. Therefore, all hydrogen in excess of 1×10^{-9} moles/milliliter of ammonia must be due to contaminants in the ammonia sample.

The reported measurements in table 5.5 represent the total amount of evolved hydrogen. Since these values may include effects due to residual contaminants on the surface as well as those tank impurities in the sodium, the data must be considered as maximum values.

TABLE 5.5
EFFECTIVENESS OF AMMONIA PURIFICATION PROCEDURES

The pyrex tubes were cleaned using the standard cleaning procedure, washed with HF Cleaner (5% HF, 33% HNO₃, 2% Alconox, 60% H₂O); rinsed with aqua regia once; rinsed with H₂O six times, then sealed onto the vacuum system and baked under vacuum at 400°C for two hours, followed by bakeout at 200° for one additional hour. The hydrogen reported includes the amount due to the contaminants in the transfer tank and the two lower results must therefore be considered as maximum values.

<u>Grade of Ammonia</u>	<u>Purification Procedure</u>	<u>Micromoles of H₂/ml NH₃</u>	<u>Micromoles of Dissolved Gases/ml NH₃</u>
Tank	Tank Ammonia	0.2	0.006
Filtered	Activated Charcoal	0.06	0.0006
Filtered and Dried	Filtered through activated charcoal, dried over Na overnight at -78°C.	0.004	0.0006
Filtered, Dried and Fractionated	(In Vacuum System), passed activated charcoal, stored over sodium overnight at -78°C, vacuum fractionated, and stored in a stainless steel cylinder	0.004	<0.0005

5.2.3 Effect of Added Contaminants

After investigating the decomposition of the sodium-ammonia solutions by contaminants already present in various parts of the system (glass walls, ammonia, and sodium), further studies were aimed at determining what types of contaminants, other than water, give rise to evolution of hydrogen by solution decomposition. This work was done by measuring the effect of various impurities added to the sample tube before reaction with the sodium-ammonia solution.

In an initial test, the effect of the presence of mercury prior to cleaning was studied. The mercury had been in contact with the glass surface and was removed by reaction with concentrated nitric acid prior to the HF cleaner treatment. No increase in the amount of evolved hydrogen was detected. Any contaminant added through the use of mercury had therefore been removed by this procedure. This result is of importance since mercury is routinely used in this laboratory for the calibration of conductivity cells.

Other impurities were tested by being placed in the tubes after cleaning but prior to bakeout. Of the various substances which were examined, NaI and CsI gave no effective increase in gas liberation over the amount due to the glass walls. A noticeable increase in decomposition was obtained with Na_2SO_4 and NaF. A stronger effect was found with tungsten wire, which had been thoroughly cleaned by electrolysis in a concentrated NaOH solution.

Salts which gave an increase in the initial reaction showed no signs of effecting solution decomposition after the 15-minute period. Tungsten, however, gave not only a high initial reaction but continued to cause decomposition even after 2 hours reaction time. The results are summarized in table 5.6.

TABLE 5.6

The pyrex tubes were cleaned using the HF cleaner followed by aqua regia and water rinses. After the impurities were added, the samples were sealed onto the vacuum system and baked under vacuum at 400°C for 2 hours, followed by an additional bakeout at 200°C for one hour. The decomposition reported is that due to added contaminants plus the contribution from the pyrex surface and is expressed in terms of an equivalent amount of water.

<u>Impurity Added</u>	<u>Molecules H₂O/sq. Å</u> <u>Glass Surface</u>
None (pyrex tube)	0.4 ± 0.2
NaI	0.5
CsI	0.4
Na ₂ SO ₄	0.7
NaF	0.8
Tungsten, 15 min. reaction time	9.0
Tungsten, 2 hr.15 min. reaction time	18.1
Tungsten, 2 hr.30 min. reaction time	22.0

During the investigation of the reactivity of added contaminants with sodium-ammonia solutions, only pyrex glass was used as the container material. Further studies were aimed at determining the contamination added by other glass types. For this purpose, uranium glass (Corning No. 3321) was chosen as the container material. In previous work, uranium glass had been examined as a container material for high temperature conductivity measurements of sodium ammonia solutions. The container invariably ruptured at about 145°C due to dissolution of the uranium glass with the solution whereas pyrex has resisted attack at temperatures up to 190°C without rupture.

The present investigation was conducted at -78°C and contrary to the high temperature results on dissolution, it was found that there was no more low temperature reaction with uranium glass than with pyrex. The reactivity was measured by the evolved hydrogen.

Additional contaminants are produced by the seal-off of the test tube, and are therefore added to the solution. These contaminants are released from the glass walls due to the high temperature required for fusing glass. The amount of contamination released during seal-off was determined using the same apparatus and techniques as for the previous investigations. In a series of tests, a number of tubes were sealed off and the non-condensable gases which evolved were measured with the combination Toepler pump-McLeod gauge. In table 5.7, the term non-condensable gases refers to those constituents which passed through two liquid nitrogen traps. In other tests, the liquid nitrogen traps were removed and the total amount of gas which evolved during seal-off was measured by the same method.

After measuring the gases released, experiments were performed to determine the amount of contaminants adherent to the glass in the seal-off region. The easily removed contaminants were pumped off at a pressure of less than 1×10^{-6} torr for 1/2 hour. Subsequently, the sodium covered bead and the ammonia were introduced. The sodium-ammonia solution reacted with contaminants producing hydrogen. The volume of evolved hydrogen is a measure of the amount of contaminants tightly bound to the glass walls and which were produced by the seal-off. In a variation of the experiment, the gases were not pumped off and thus all impurities produced during seal-off could react with the sodium-ammonia solution. This last measurement is

an indication of the total amount of contaminants which is produced during the sealing process and is contained in the sealed off tube.

Various procedures were used for the seal-off. In some cases, extensive preheating was used prior to seal-off while a pressure of less than 1×10^{-6} torr was maintained. Other tubes were sealed off such that the glass was near the fusing point for a minimum of time. Preheating appeared to have no effect on the amount of released contaminants except in the case of heating the samples to the softening point for a period of more than one hour. In this case, the tubes almost completely collapsed, but seal-off contamination was reduced. However, a prolonged bakeout at 400°C was even more effective in reducing seal-off contaminants. All other seal-off variations such as changing flame or annealing temperature had no noticeable effect on the amount of evolved contaminants. The results of the investigation are summarized in table 5.7.

TABLE 5.7
SEAL-OFF CONTAMINATION

	Seal-Off			No Seal-off
	2-Hr. 400°C 1-Hr. 200°C Bakeout	200-Hr. 400°C Bakeout	1-Hr. 550°C Bakeout	2-Hr. 400°C 1-Hr. 200°C Bakeout
Non-Condensable gases evolved during seal-off (micromoles)	0.015	0.002	0.005	--
Total gases evolved during seal-off (Micromoles)	0.06*	0.009	0.03	--
H ₂ evolved from Na-NH ₃ reaction in seal-off region (Micromoles)	0.15 (pumped after seal-off)	--	--	0.03
Total contaminants released during seal-off in terms of H ₂ evolved from reaction in seal-off region (no pumping during or after seal-off) (Micromoles)	1.0	--	--	--

*This is a minimum value rather than an actual value since the final pressure in the McLeod gauge at reading was about 40 mm Hg whereas the vapor pressure of water at 25° is only 24 mm Hg. Part of the evolved water could have condensed in the gauge and might not have been detected.

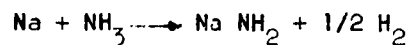
Blank spaces in the table indicate either no data yet available or heading is not applicable.

5.3 CONCLUSIONS

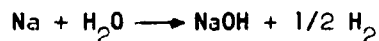
Quantitative measurements have been made to determine the effectiveness of various cleaning procedures. By means of these measurements, a cleaner consisting of 5% HF, 33% HNO₃, 2% Alconox and 60% H₂O has proven to leave the least amount of residue which reacts with sodium-ammonia solution. This cleaner is most effective when followed by an aqua regia rinse and numerous distilled-water rinses.

If this procedure is used, a prolonged 200-hour bakeout at 400°C as proposed by Warshawsky decreases only very slightly the amount of "water" left on the surface. An increase in bakeout temperature up to 500°C has no noticeable effect on the amount of residual contaminants. This prolonged or higher temperature bakeout might be more effective with another type of cleaner.

It has been shown that added impurities such as NaI and CsI do not contribute to the initial decomposition of the sodium-ammonia solution. These added contaminants may catalyze the slower, long-range decomposition but do not measurably affect the decomposition during the 15-minute test period. Tungsten, however, does contribute to the initial reaction and the reaction is still continuing after more than 2 hours. This is probably due to the catalytic effect of the tungsten on the normal decomposition reaction of sodium-ammonia solutions:



as well as to a contribution to the initial or Warshawsky decomposition which is nominally expressed in the form:



We have shown that tank ammonia is quite impure for the purpose of making stable metal-ammonia solutions. However, most of the dissolved gases are absorbed by passing through activated charcoal while any water content is removed by storage on sodium metal overnight at -78°C . After this purification, subsequent fractionation adds slightly to the purity of the ammonia. A slight reaction of ammonia with sodium occurs which lasts for a short time. After this reaction, a sodium-ammonia solution is formed which is very stable.

5.4 PROGRAM FOR THE NEXT PERIOD

During the next period, additional tests will be performed in order to determine the role of each ingredient in the HF cleaner. More added contaminants and different glasses will also be tested. In addition, tests will be made to fill in gaps in the present data. The results are being prepared for publication and the tests should be completed during the next interval.

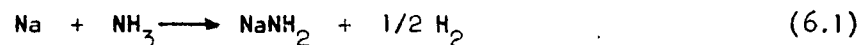
5.5 REFERENCES

- 5.1 I. Warshawsky, J. Inorg. Nucl. Chem. 25, 601 (1963).
- 5.2 Progress Report of August 19, 1964.
- 5.3 R. H. A. Crawley, Chem. and Ind. 45, 1205 (1953).

6.0 CHEMICAL ANALYSIS OF SODIUM-AMMONIA SOLUTIONS AND SOLUBILITIES OF SALTS

6.1 INTRODUCTION

From the inception of the program, it was recognized that chemical analysis should be used to back up the physical data obtained from sodium-ammonia solutions, such as conductivity by the induction method. Current practice is to measure the conductivities at low temperature and relate those to the data by Kraus^(6.1). On the other hand, the extent of any amide formation, according to the equation



can be measured by a gas-volumetric method. The questions about the stability of sodium-ammonia solutions can be answered by chemical analysis. Similarly, the stability in the presence of salts can be investigated. At the same time the question arose as to whether the solubility of salts in sodium-ammonia solutions could be significantly different from that in pure ammonia.

6.2 EXPERIMENTAL

6.2.1 Chemical Analysis

The need for a chemical determination of the composition of the sodium-ammonia solutions was met by constructing an apparatus called, in the following, the gas analyzer (figure 6.1).

The design avoids passage of gaseous or solid ammonia through the traps with the stream of hydrogen gas. This would increase the measured gas quantity above that of the amount of hydrogen present. The samples were broken at the temperature of liquid nitrogen to avoid reaction on warm metal surfaces.

For the analysis, samples were broken in the highly evacuated cylinder, and the free hydrogen was gradually released through the two traps at -196° toward the manometer line. After compressing the entire quantity of gas, using the Toepler pump, a reading of volume, pressure and temperature was taken.

Next, the frozen ammonia was melted down in trap 1, the trap was surrounded with crushed dry ice and after 5 minutes, a reading of the liquid volume at the freezing point (-78°C) was taken (± 0.02 ml accuracy).

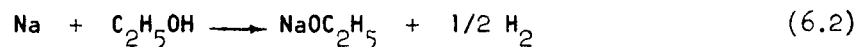
Ethanol (10 ml) was added through the funnel to the steel cylinder containing the sodium. Using the valve and stopcock before trap 1, the evolved hydrogen was slowly released through the traps at -196° to the measuring volume, compressed by means of the Toepler pump, and then measured.

The steel cylinder containing sodium ethoxide was taken off, opened to the atmosphere, and washed three times with distilled water while holding back the steel ball and broken glass with a filtration funnel. The solution or part of it (1/5 or 1/10) was titrated using 0.1 N HCl and phenolphthalein.

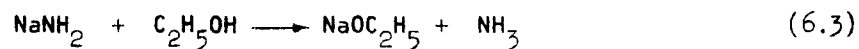
The obtained data are: (1) initial hydrogen, (2) hydrogen from sodium and ethanol, (3) total base, and (4) free ammonia.

These quantities are the subject of the following discussion. Initial hydrogen may stem mostly from the reaction represented by equation (6.1). Small values of initial hydrogen indicate that the solution

has not significantly reacted to form the amide. Reaction of sodium and ethanol releases hydrogen according to equation (6.2):



Besides, the amide from equation (6.1) reacts according to equation (6.3):



This quantity of ammonia, together with the free ammonia, would give the total ammonia in the sample. It can be obtained by distilling the alcohol into the detachable trap 2, diluting with water and titrating, using standardized HCl and a suitable indicator. Total base (NaOH) represents probably quite well the initial quantity of sodium in the sodium-ammonia solution. One would expect that this quantity should be double that of the total hydrogen; but in practice one finds slightly excessive gas quantities. This problem is still under study.

Table 6.1 contains representative data of chemical analysis and some corresponding conductivity data. The maximal temperatures are listed to which the samples were exposed during the conductivity measurements.

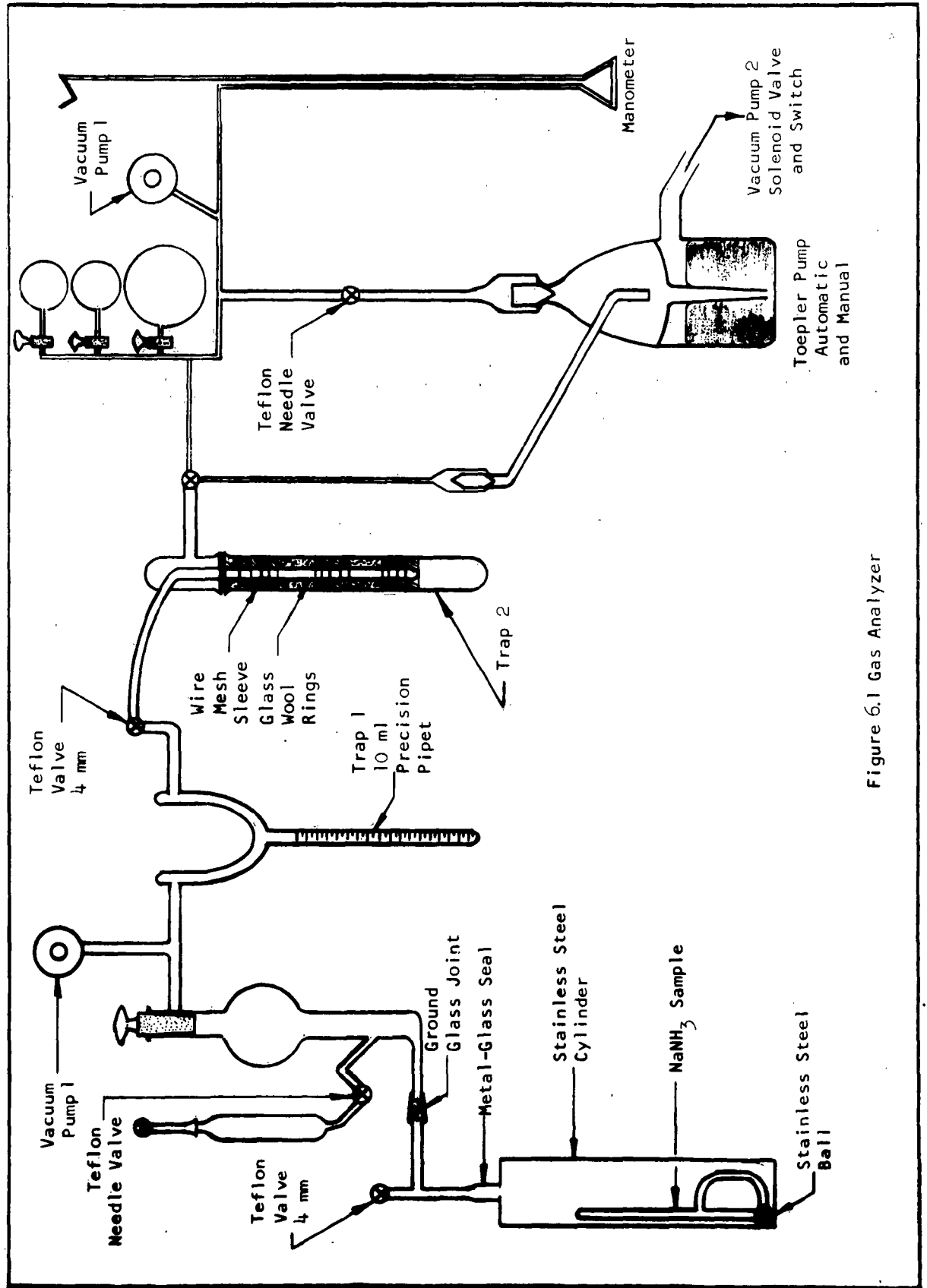


Figure 6.1 Gas Analyzer

TABLE 6.1

Sample No.	Highest Temp. °C	Number of Heatings	σ^* mho/cm	Volume Liquid NH_3 , ml -78°C	Millimoles				Mole % of Sodium			Remarks
					H_2 Init.	H_2 Total	NaOH	Free NH_3	Total H_2	Total Minus Initial H_2	NaOH	
183	140	1	16.5	5.3	.531	3.00	6.15	2.56	2.12	2.63	3.10	
192	62	1	6.85	6.5	.272	3.58	6.75	2.49	2.31	2.36	2.64	
149	60	1	---	7.0	.144	.201	0.310	0.133	0.038	0.103	---	
250	60	1	2,730	5.35	.233	13.91	26.65	10.89	10.6	10.4	12.0	
253	60	1	1,460	5.35	.204	11.36	21.50	8.99	8.85	8.53	9.40	
231	160	2	76.0	4.09	.224	4.15	6.00	4.50	4.27	3.30	3.97	
245	60	1	---	6.55	.040	0.32	0.75	0.23	0.20	0.266	---	
258	103	3	4,600	4.65	0.100	(15.6 ^{***})	36.45	(13.5 ^{***})	(13.4 ^{***})	15.4	15.	Excess Na

*All specific conductivities at -33.5°C .

***Not enough ethanol was added to react with all the sodium present.

6.2.2 Solubility of Salts

A series of experiments was initiated for the purpose of studying the stability of sodium-ammonia solutions in the presence of salts. In the first experiment the following bakeable and ammonia-insoluble salts were chosen: sodium fluoride, sodium carbonate, and sodium sulfate. Ampoule cells were charged with a salt quantity corresponding to about 0.1 equivalent of sodium ion per liter, baked and charged with sodium and ammonia in the usual manner. Conductivity was measured descending from room temperature to the point of phase separation. The cell was then broken in vacuo for the chemical analysis. Table 6.2 contains representative data of several experiments. Sodium fluoride and carbonate gave considerable quantities of initial hydrogen and appear to have caused some amide formation. Sodium sulfate on the other hand shows quite normal values of initial hydrogen. No appreciable increase in solubility was observed; the salts are regarded as quite insoluble in pure ammonia.

The studies are being extended to include soluble salts such as sodium iodide and insoluble salts containing no sodium ion.

TABLE 6.2

Sample No.	Salt	Phase Sep. Temp.		Highest Temp.	σ^* $\mu\text{ho/cm}$	Volume Liquid NH_3 , ml -78°C	Millimoles				Mole %				
		Run	Lit				Na^+ From Salt	H_2 Init.	H_2 Total	NaOH	NH_3	Total H_2	Total minus Init. H_2	NaOH	Cond.
254	Na_2SO_4	--	--	Room	3,150	3.5	0.662	0.475	11.16	21.15	151	12.8	12.3	12.2	12.7
252	Na_2SO_4	-44°	-45°	Room	334	5.0	0.633	0.118	6.44	11.95	215	5.61	5.51	5.22	5.57
238	Na_2CO_3	--	--	Room	1,380	4.1	0.592	4.526	7.93	13.90	177	8.18	3.68	7.25	9.2
237	NaF	-45°	-43.5°	Room	17.3	5.5	0.617	3.385	3.91	7.30	237	3.15	0.44	2.97	3.22
235	NaF	--	--	Room	2.1	6.3	0.531	0.269	2.49	4.53	271	1.78	1.58	1.64	2.08

specific conductivities at -33.5°C .

6.3 CONCLUSIONS

Useful procedures for the determination of the chemical composition of sodium-ammonia solutions have been developed and are being improved. The results in table 6.1 show the stability of sodium-ammonia solutions up to 160°C. It is further shown in table 6.2 that decomposition may not take place in presence of some salts (Na_2SO_4) and may vary considerably for a given salt (NaF).

6.4 PROGRAM FOR THE NEXT PERIOD

Future plans involve improving the reliability of the analytical procedure, study of the sources of excessive hydrogen gas, such as side reactions with ammonia, and the behavior of salts, both soluble and insoluble, with large cations. Further work will be carried out on the relation of conductivity data to base titration data. Certain observations indicate that indeed unusual solubilities and effects of salts are possible, for instance, barium carbonate, BaCO_3 , appears to be soluble in concentrated sodium-ammonia solution.

6.5 REFERENCES

(6.1) C. A. Kraus and W. W. Lucasse, J. Am. Chem. Soc., 45, 2551 (1923)

UNCLASSIFIED

Security Classification

DOCUMENT CONTROL DATA - R&D

(Security classification of title, body of abstract and indexing annotation must be entered when the overall report is classified)

1. ORIGINATING ACTIVITY (Corporate author) UNIFIED SCIENCE ASSOCIATES, INC. 326 South Arroyo Parkway Pasadena, California 91105		2a. REPORT SECURITY CLASSIFICATION UNCLASSIFIED	
		2b. GROUP	
3. REPORT TITLE STABLE DENSE COLD PLASMA			
4. DESCRIPTIVE NOTES (Type of report and inclusive dates) Semiannual Report, 20 August 1964 through 19 February 1965			
5. AUTHOR(S) (Last name, first name, initial) Naiditch, S.			
6. REPORT DATE April 1965	7a. TOTAL NO. OF PAGES 66	7b. NO. OF REFS 12	
8a. CONTRACT OR GRANT NO. NONR 3437(00)		9a. ORIGINATOR'S REPORT NUMBER(S) C-3	
b. PROJECT NO. Order No. 194, Amendment No. 5			
c. Program Code No. 4980		9b. OTHER REPORT NO(S) (Any other numbers that may be assigned this report)	
10. AVAILABILITY/LIMITATION NOTICES All distribution of this report is controlled. Qualified DDC users shall request through Office of Naval Research, Washington, D. C.			
11. SUPPLEMENTARY NOTES		12. SPONSORING MILITARY ACTIVITY Department of the Navy, Office of Naval Research	
13. ABSTRACT The purpose of this contract is to conduct research on chemical and physical properties of sodium ammonia solutions relating to their plasma aspects. During the period of this report chemical studies were conducted in order to increase the lifetime of the solutions at elevated temperatures. This work included investigating effects of surface contaminants and solvent purification on the decomposition of sodium ammonia solutions. Quantitative measurements have been made to determine the effectiveness of various cleaning procedures for glass surfaces. A search was conducted for contaminants other than water which cause decomposition of the solution. Among the investigated contaminants, tungsten had the strongest effect. Procedures for chemical analysis of sodium ammonia solutions were developed. The analysis confirmed the stability of sodium ammonia solutions up to 160°C and agreed fairly well with our conductivity data. Studies on salts in contact with sodium ammonia solutions were carried out. The electrodeless Hall effect apparatus under development to provide data on electron densities and mobilities, was used to measure the Hall coefficient of mercury. This experiment was primarily considered as a final test of the apparatus. Unexpected difficulties were encountered from pickup noise and intermodulation. It was possible to overcome the disturbing effects on the measuring circuit			

DD

FORM
1 JAN 64

1473

0101-807-6800

UNCLASSIFIED

Security Classification

13. ABSTRACT continued

sufficiently that Hall effect measurements on a cell with electrodes could be performed. The measured result was in fairly good agreement with the literature.

An apparatus for measuring magnetic susceptibilities of sodium ammonia solutions was devised. The functioning of the apparatus was tested by measuring the magnetic susceptibility of distilled water. First measurements on ammonia and sodium ammonia solutions were performed at room temperatures.

14. KEY WORDS	LINK A		LINK B		LINK C	
	ROLE	WT	ROLE	WT	ROLE	WT
Chemical and physical properties of sodium ammonia solutions. Plasma aspects. Lifetime of solutions at elevated temperatures. Surface contaminants. Solvent purification. Cleaning procedures for glass surfaces. Catalytic effect of tungsten. Chemical analysis. Electrodeless Hall effect measurement. Magnetic susceptibility measurement.						

INSTRUCTIONS

1. **ORIGINATING ACTIVITY:** Enter the name and address of the contractor, sub-contractor, grantee, Department of Defense activity or other organization (*corporate author*) issuing the report.
- 2a. **REPORT SECURITY CLASSIFICATION:** Enter the overall security classification of the report. Indicate whether "Restricted Data" is included. Marking is to be in accordance with appropriate security regulations.
- 2b. **GROUP:** Automatic downgrading is specified in DoD Directive 5200.10 and Armed Forces Industrial Manual. Enter the group number. Also, when applicable, show that optional markings have been used for Group 3 and Group 4 as authorized.
3. **REPORT TITLE:** Enter the complete report title in all capital letters. Titles in all cases should be unclassified. If a meaningful title cannot be selected without classification, show title classification in all capitals in parenthesis immediately following the title.
4. **DESCRIPTIVE NOTES:** If appropriate, enter the type of report, e.g., interim, progress, summary, annual, or final. Give the inclusive dates when a specific reporting period is covered.
5. **AUTHOR(S):** Enter the name(s) of author(s) as shown on or in the report. Enter last name, first name, middle initial. If military, show rank and branch of service. The name of the principal author is an absolute minimum requirement.
6. **REPORT DATE:** Enter the date of the report as day, month, year, or month, year. If more than one date appears on the report, use date of publication.
- 7a. **TOTAL NUMBER OF PAGES:** The total page count should follow normal pagination procedures, i.e., enter the number of pages containing information.
- 7b. **NUMBER OF REFERENCES:** Enter the total number of references cited in the report.
- 8a. **CONTRACT OR GRANT NUMBER:** If appropriate, enter the applicable number of the contract or grant under which the report was written.
- 8b, 8c, & 8d. **PROJECT NUMBER:** Enter the appropriate military department identification, such as project number, subproject number, system numbers, task number, etc.
- 9a. **ORIGINATOR'S REPORT NUMBER(S):** Enter the official report number by which the document will be identified and controlled by the originating activity. This number must be unique to this report.
- 9b. **OTHER REPORT NUMBER(S):** If the report has been assigned any other report numbers (*either by the originator or by the sponsor*), also enter this number(s).
10. **AVAILABILITY/LIMITATION NOTICES:** Enter any limitations on further dissemination of the report, other than those imposed by security classification, using standard statements such as:
- (1) "Qualified requesters may obtain copies of this report from DDC."
 - (2) "Foreign announcement and dissemination of this report by DDC is not authorized."
 - (3) "U. S. Government agencies may obtain copies of this report directly from DDC. Other qualified DDC users shall request through _____."
 - (4) "U. S. military agencies may obtain copies of this report directly from DDC. Other qualified users shall request through _____."
 - (5) "All distribution of this report is controlled. Qualified DDC users shall request through _____."
- If the report has been furnished to the Office of Technical Services, Department of Commerce, for sale to the public, indicate this fact and enter the price, if known.
11. **SUPPLEMENTARY NOTES:** Use for additional explanatory notes.
12. **SPONSORING MILITARY ACTIVITY:** Enter the name of the departmental project office or laboratory sponsoring (*paying for*) the research and development. Include address.
13. **ABSTRACT:** Enter an abstract giving a brief and factual summary of the document indicative of the report, even though it may also appear elsewhere in the body of the technical report. If additional space is required, a continuation sheet shall be attached.
- It is highly desirable that the abstract of classified reports be unclassified. Each paragraph of the abstract shall end with an indication of the military security classification of the information in the paragraph, represented as (TS), (S), (C), or (U).
- There is no limitation on the length of the abstract. However, the suggested length is from 150 to 225 words.
14. **KEY WORDS:** Key words are technically meaningful terms or short phrases that characterize a report and may be used as index entries for cataloging the report. Key words must be selected so that no security classification is required. Identifiers, such as equipment model designation, trade name, military project code name, geographic location, may be used as key words but will be followed by an indication of technical context. The assignment of links, roles, and weights is optional.

ABSTRACT

An analysis of the two transformer system is presented. It is found that there is a frequency region in which the voltage transfer is proportional to the sample conductance. A comparison is made between the measured and predicted behavior of a two transformer system. The good agreement obtained indicates that the method of analysis can be used as an aid to designing two transformer conductivity measuring systems.

THE TWO TRANSFORMER METHOD FOR
ELECTRODELESS CONDUCTIVITY MEASUREMENT*

R. A. Williams, E.M. Gold⁺ and S. Naiditch
Unified Science Associates, Inc., Pasadena, California

INTRODUCTION

In cases where it is desired to measure the conductivity of liquids which are chemically unstable in the presence of metals, the two transformer principle for electrodeless conductivity measurement is often used¹⁻⁵. The usual application of this principle involves a nulling technique in which the voltage transferred from the input to the output coils by means of the sample loop is balanced against a similar voltage transferred by means of a loop of known resistance. Although such null methods make possible the attainment of high precision, the complication involved is unnecessary when accuracies of a few percent are sufficient. In such cases, it is necessary only to measure the voltage transfer across the two transformer system because, under the proper conditions, this transfer is directly proportional to the conductance of the sample being studied. For example, Naiditch has used this direct technique to measure the conductivities of sodium ammonia solutions at elevated temperatures⁶. Also, a commercial unit of this type is available (Industrial

*Supported by the Advanced Research Projects Agency and the Office of Naval Research under Contract No. NONR-3437(00).

⁺Presently at Sloan Mathematics Center, Stanford University, California.

- 1 M. J. Relis, U. S. Patent No. 2542057 (1951).
- 2 J. E. Fielden, U. S. Patent No. 270985 (1955).
- 3 S. R. Gupta and G. H. Hills, J. Sci. Instr. 33, 313 (1956).
- 4 R. Calvert, J. A. Cornelius, V. S. Griffiths, and D. I. Stock, J. Phys. Chem. 62, 47 (1958).
- 5 I. Fatt, Rev. Sci. Inst. 33, 493 (1962).
- 6 G. Lepoutre and M. J. Sienko, Metal-Ammonia Solutions (Benjamin, 1964), pp. 113-136.

Instruments, Inc., Cedar Grove, New Jersey). The purpose of this paper is to evaluate both theoretically and experimentally the behavior of a two transformer system with particular regard to the constant of proportionality and the conditions under which proportionality exists. This information should aid in the design of electrodeless conductivity measuring systems of both the bridge and voltage transfer types.

ANALYSIS

Figure 1 shows the elements of the two transformer system. Two identical toroidal coils wound on ferromagnetic cores are linked by a closed loop of the liquid to be measured. The tubing for this loop must be both non-magnetic and an insulator and is commonly of glass. The input coil is driven by an oscillator and induces a voltage in the sample loop. A current which depends on the resistance of the sample is therefore made to flow in the loop, and this current in turn induces a voltage on the output coil where it can be measured with a VTVM.

Figure 2 shows a schematic diagram of the system which includes those elements which are necessary to account for the observed behavior of the system. In this diagram, the sample is represented by its resistance R and its free space inductance L_0 . Since the sample encircles two toroidal, ferromagnetic cores, it has for each of these an additional inductance L_1 equal to the inductance of a single turn around such a core. The input coil has n turns and is represented by its inductance $L_n = n^2 L_1$ plus a resistance, r , to represent losses in the input coil. These losses include hysteresis, eddy currents, and electromechanical losses in addition

to the ohmic losses in the wire. The output coil also has n turns so that its inductance is L_n . Losses in the output coil will be neglected as they have very little effect since practically no current flows in the output circuit. The capacity C of the output circuit includes the input capacity of the VTVM and the capacity of the cable between the coil and the VTVM as well as the stray capacity in the coil itself.

We define a coupling constant K so that of the total magnetic flux generated by one of the toroidal coils, K is the fraction which passes through the sample loop.

The equations for the four loops of the system are then

$$V_i = I_1(r + Z_n) - K I_2 \sqrt{Z_1 Z_n}$$

$$0 = I_2(R + Z_o + 2Z_1) - K I_1 \sqrt{Z_1 Z_n} - K I_3 \sqrt{Z_1 Z_n}$$

$$V_o = I_3 Z_n - I_2 K \sqrt{Z_1 Z_n}$$

$$V_o = -I_3 Z_c$$

where the subscripts i and o refer to input and output, respectively, and where, at a frequency ν , $Z_1 = j2\pi\nu L_1$, $Z_n = n^2 Z_1$, $Z_o = j2\pi\nu L_o$ and $Z_c = -j/2\pi\nu C$ with $j = \sqrt{-1}$. The above can be solved to yield the ratio of output to input voltage.

$$\frac{V_o}{V_i} = - \left\{ \left(1 + \frac{Z_n}{Z_c}\right) \left[\left(1 + \frac{r}{Z_n}\right) \frac{R + Z_o + 2Z_1}{K^2 Z_1} - 1 \right] - \left(1 + \frac{r}{Z_n}\right) \frac{Z_n}{Z_c} \right\}^{-1}$$

It is instructive to examine the asymptotic frequency response of the function $F = \left| \frac{V_o}{V_i} \right| \cdot \frac{R}{\nu}$ which is a constant in the frequency region most suited

to conductance measurement. At low frequencies, the resistance of the input coil dominates, $r \gg Z_n$, $R \gg Z_o + 2Z_1$ and $Z_c \gg Z_n$ so that

$$F = K^2 4\pi^2 n^2 L_1^2 \cdot v/r$$

At intermediate frequencies, the loop resistance is the dominant factor

$r \ll Z_n$, $R \gg Z_o + 2Z_1$, $Z_c \gg Z_n$ and F is constant

$$F = K^2 2\pi L_1$$

At higher frequencies the loop inductance becomes dominant

$r \ll Z_n$, $R \ll Z_o + 2Z_1$, $Z_c \gg Z_n$ giving

$$F = \left[K^2 L_1 / (L_o + 2L_1 - K^2 L_1) \right] \cdot R/v$$

At still higher frequencies the output capacity dominates and

$r \ll Z_n$, $R \ll Z_o + 2Z_1$, $Z_c \ll Z_n$ so that

$$F = \frac{K^2 R}{4\pi^2 n^2 C \left[L_o + 2L_1 (1-K^2) \right]} \cdot \frac{1}{v^3}$$

In addition there is a resonance near $Z_n/Z_c = -1$ or near the frequency $v_o = 1/(2\pi \sqrt{L_1 C})$. Actually, the resonant frequency depends on the sample resistance R and varies from v_o at $R = \infty$ to $v_o \left[(L_o + 2L_1 - K^2 L_1) / (L_o + 2L_1 - 2K^2 L_1) \right]^{1/2}$ at $R = 0$. For large R the input and output voltages are equal at resonance while for small R the peak value is determined by the losses in the output coil. The resonance is of interest, however, only in that it should be avoided. The best frequencies for conductivity measurement are those in the second region (where F is constant), for here the voltage transfer is proportional to the conductance of the sample being studied and depends only on the first power of the frequency.

EXPERIMENTAL STUDY

As a test of the foregoing analysis, the frequency response of a two transformer system was measured for various resistances in the sample loop. The input and output coils were thirty three turns of No. 26 enameled copper wire wound on toroidal cores of Q_1 ferramic and having a 3.2 cm outside diameter and with square cross section of 0.64 cm on each side. The output coil was shielded with 3 mm of copper so that it would be free of background picked up from the input coil and external sources such as nearby electrical equipment. The input coil was unshielded and was driven by a Knight audio oscillator with a transformer to match the very low impedance of the input coil to the output of the oscillator. This matching was ineffective at low frequencies so that appreciable distortion of the oscillator waveform occurred below 600 cps. The input and output voltages were measured using Hewlett-Packard 400D VTVM's while the frequency was measured with a General Radio 1142-A Frequency Meter.

Figure 3 shows the frequency response of the two transformer system with various values of the loop resistance. Rather than plotting the voltage transfer against frequency, we have plotted the function $F(\nu)$ defined earlier. The curves for the various resistances all have a range corresponding to the second region where $F(\nu)$ is constant at a value of 4.4×10^{-7} ohm sec/cycle. The flat region of the curves overlap for a wide range of resistance so that, in the present example, at a frequency of 5 KC the voltage transfer is inversely proportional to the sample resistance for the range between 0.03 ohm and 10 ohms. The range of

proportionality at various frequencies can be seen from Figure 4. Theoretically, in this region $F = K^2 2\pi L_1$ so that

$$K^2 L_1 = 7 \times 10^{-8} \text{ henries.}$$

The predicted value of L_1 for the toroids used is 8.1×10^{-8} henries, suggesting that the coupling constant has the value $K = 0.93$.

For a detailed consideration of the other aspects of the frequency response curve, consider Figure 5 which shows the measured values of $F(v)$ with a 2.54 cm by 7.62 cm rectangle of No. 26 copper wire as the sample. This loop has a resistance $R = 0.027$ ohm and its inductance is calculated theoretically to be $L_0 = 16.6 \times 10^{-8}$ henries. The output cable is 4.47 m of RG 58-U having a capacity of 4.18×10^{-10} farads. To this must be added the 15 μf stray capacity between the output coil and its grounded shield. Thus, the total output capacity is $C = 4.4 \times 10^{-10}$ farads. The input coil contains 94 cm of No. 26 copper wire. Neglecting hysteresis and eddy current losses, the input resistance is then 0.13 ohm.

Using $K = 0.93$, the theoretical asymptotes are therefore as plotted on Figure 5 and are seen to be in excellent agreement with the measured curve except at frequencies below 300 cps. This disagreement is due to noise and to distortion caused by overload of the oscillator at low frequencies.

DISCUSSION

From Figures 3 and 4 it can be seen that there exists a frequency region where the voltage transfer of the two transformer system is proportional to the sample conductance over a wide range of conductances. Thus,

the method provides a simple and reliable means of measuring the conductivity of highly corrosive liquids. In the present case, the accuracy of the conductivity measurement is limited by the accuracy of the instruments measuring input and output voltages and the frequency, and is of the order of several percent. The flatness of the $F(\nu)$ curves in the proportional region indicates, however, that high accuracies might be obtainable through the use of highly accurate voltage and frequency measuring devices.

From Figure 5 it is evident that the theoretical model presented here is adequate to explain the observed behavior of the two transformer system, the agreement being good except at low frequencies where noise and waveform distortion cause a marked deviation. More complex models may often be desirable, however, as the present case is somewhat simplified in that the input and output coils as well as the coupling constants for the input and output are identical. In any case, the use of such a model should simplify the design of two transformer systems having the particular characteristics needed for a given conductivity measuring problem.

Figure Captions

Fig. 1 Two Transformer Conductivity Gauge

Fig. 2 Schematic of Two Transformer System

Fig. 3 Frequency Response for Various Sample Resistances

Fig. 4 Range of Proportionality at Different Frequencies

Fig. 5 Comparison of Theoretical and Observed Frequency Response for $R = 0.027$

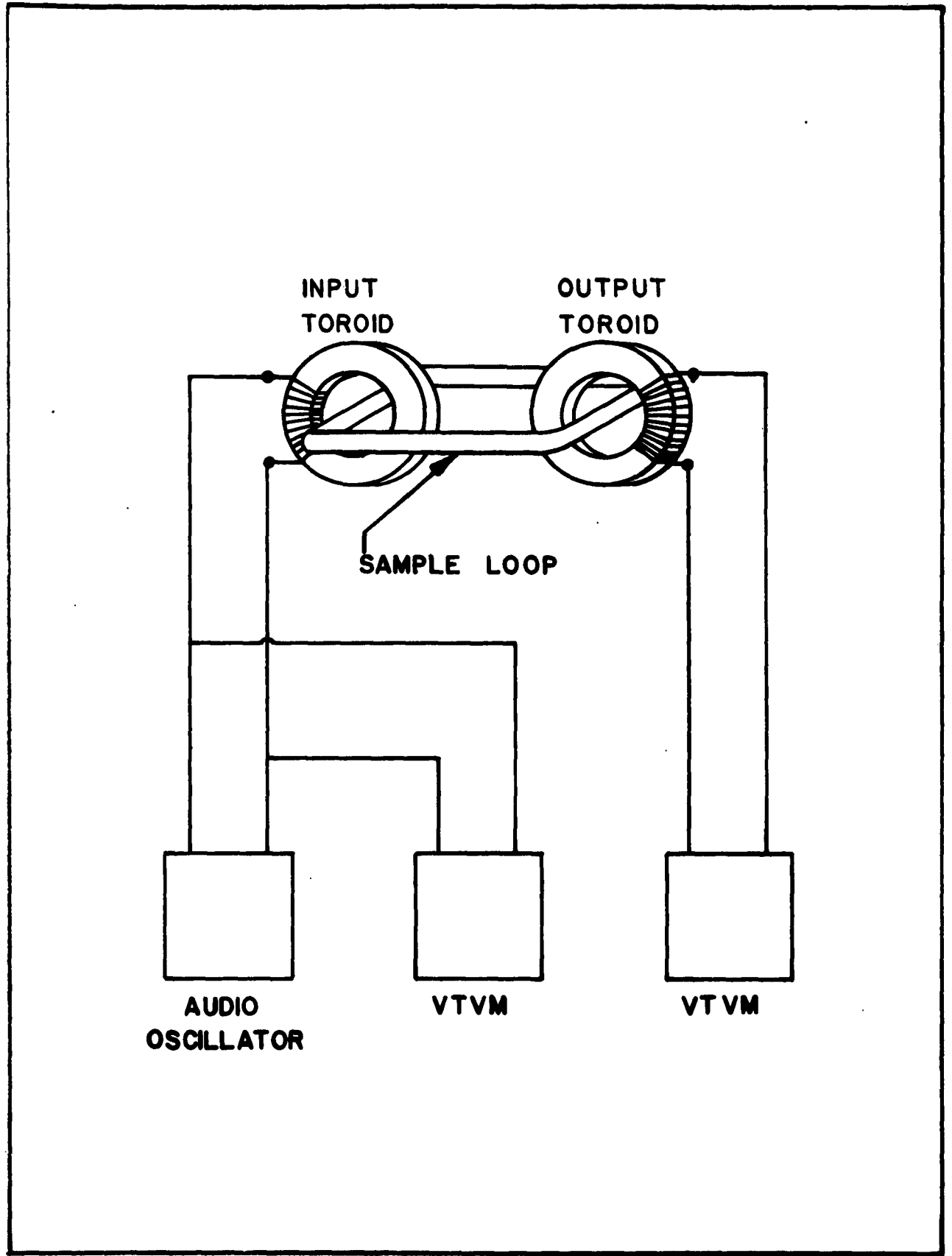
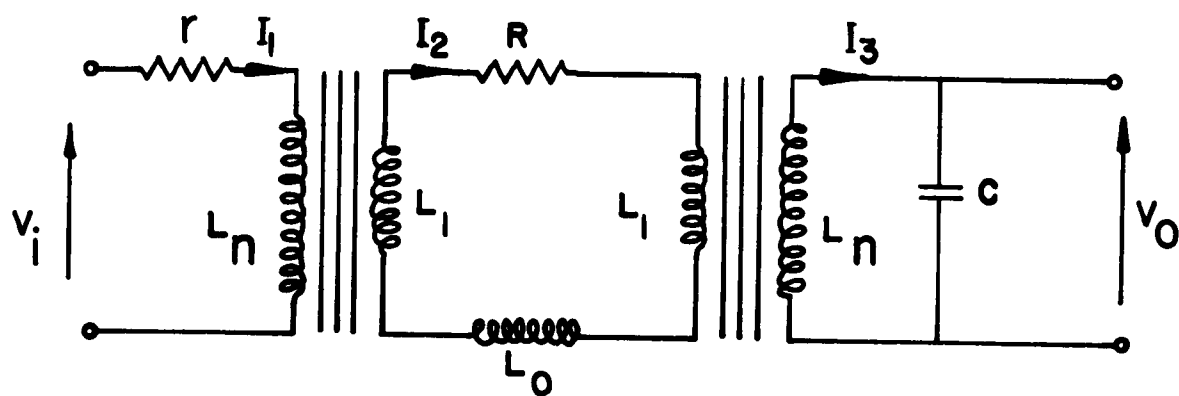


FIGURE 1

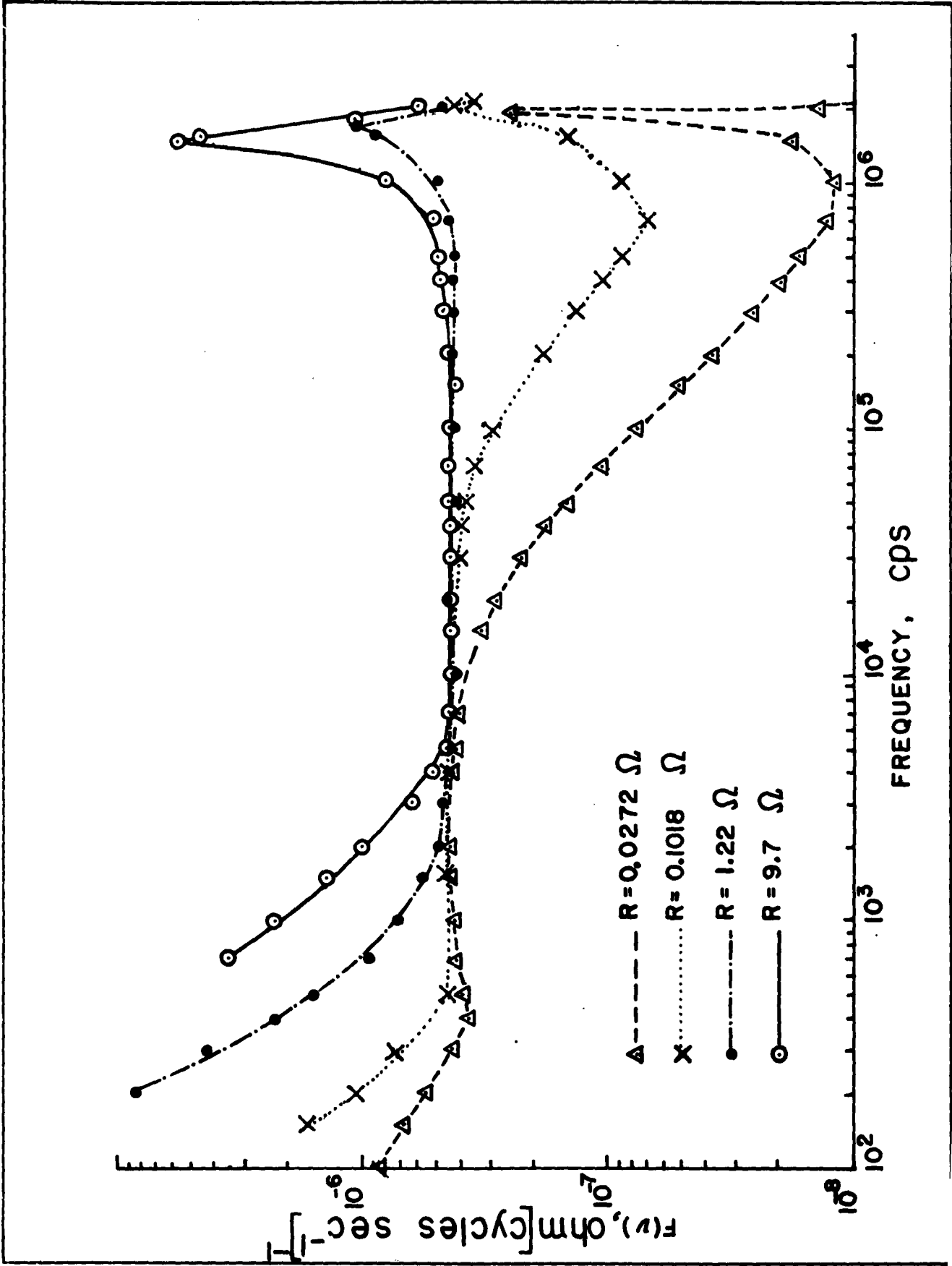


INPUT

SAMPLE LOOP

OUTPUT

FIGURE 2



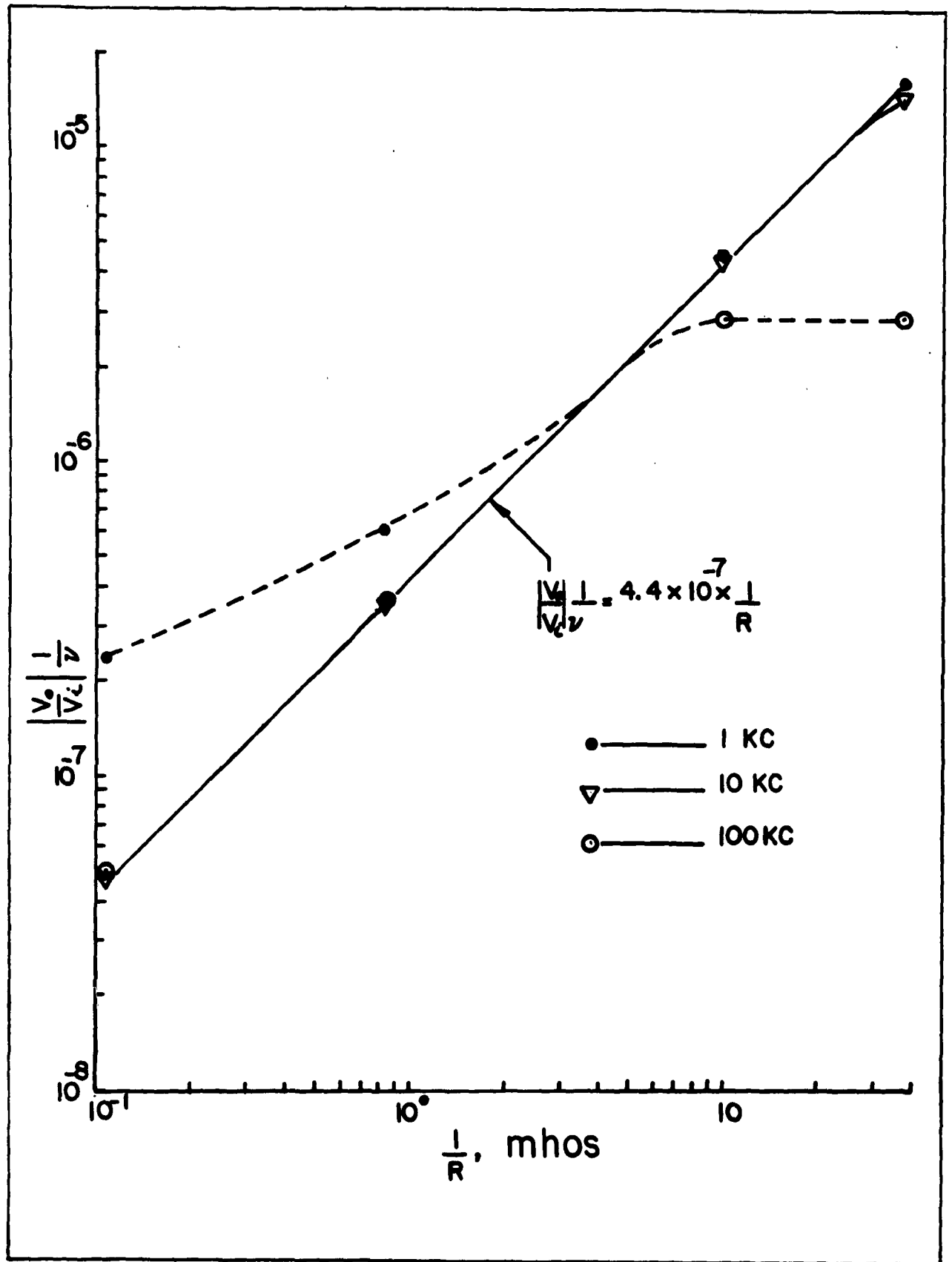


FIGURE 4

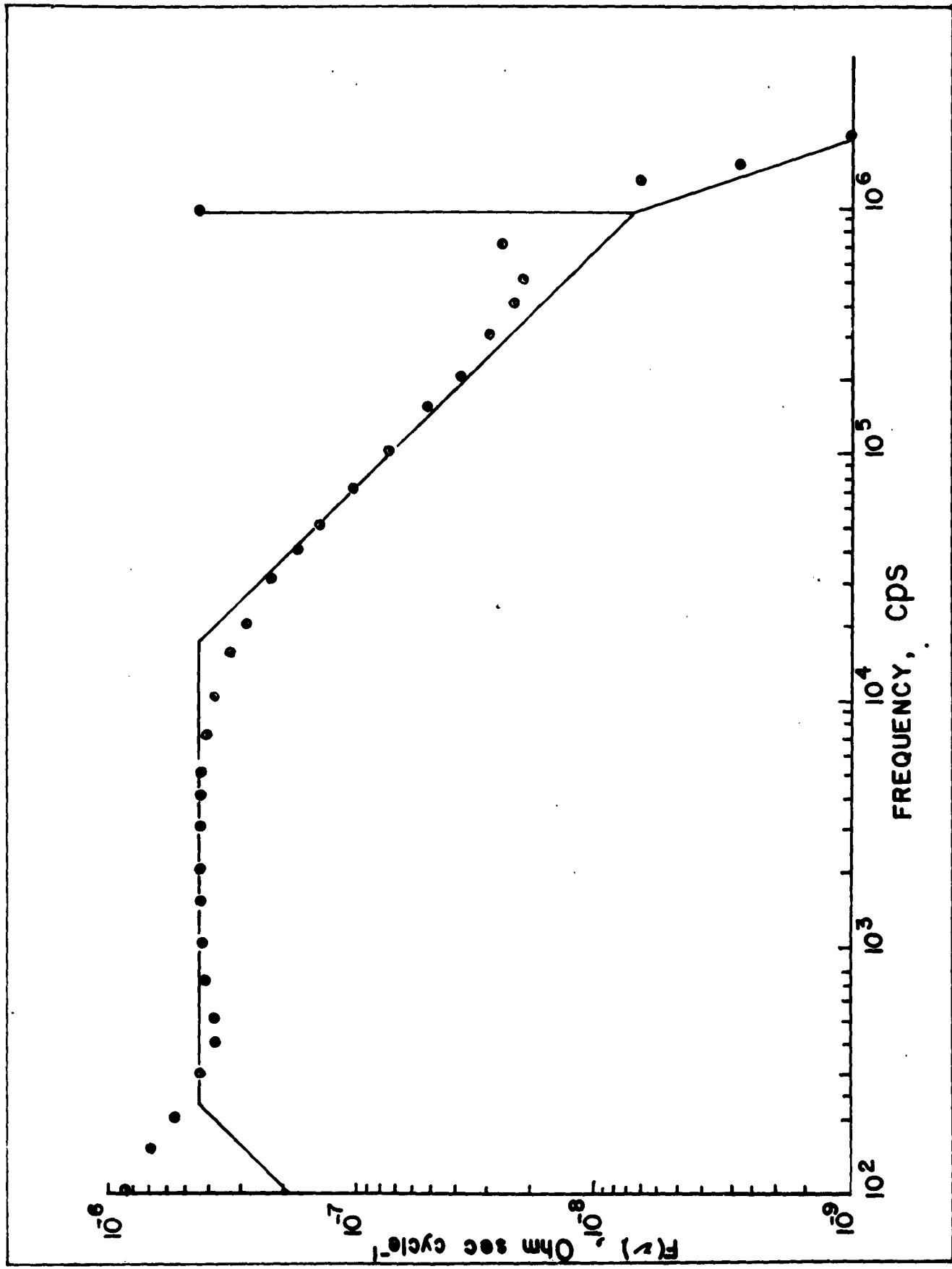


FIGURE 5